Chemical Science

ROYAL SOCIETY OF CHEMISTRY

PERSPECTIVE

View Article Online
View Journal | View Issue

Cite this: *Chem. Sci.*, 2021, **12**, 7214

All publication charges for this article have been paid for by the Royal Society of Chemistry

Received 31st March 2021
Accepted 13th May 2021

DOI: 10.1039/d1sc01827b

rsc.li/chemical-science

Beyond structural motifs: the frontier of actinide-containing metal–organic frameworks†

Corey R. Martin, Gabrielle A. Leith and Natalia B. Shustova *

In this perspective, we feature recent advances in the field of actinide-containing metal–organic frameworks (An-MOFs) with a main focus on their electronic, catalytic, photophysical, and sorption properties. This discussion deviates from a strictly crystallographic analysis of An-MOFs, reported in several reviews, or synthesis of novel structural motifs, and instead delves into the remarkable potential of An-MOFs for evolving the nuclear waste administration sector. Currently, the An-MOF field is dominated by thorium- and uranium-containing structures, with only a few reports on transuranic frameworks. However, some of the reported properties in the field of An-MOFs foreshadow potential implementation of these materials and are the main focus of this report. Thus, this perspective intends to provide a glimpse into the challenges, triumphs, and future directions of An-MOFs in sectors ranging from the traditional realm of gas sorption and separation to recently emerging areas such as electronics and photophysics.

Introduction

The fundamental understanding of properties of actinide (An)-containing materials[1,2] is paramount for nuclear waste storage, separation, and efficient reprocessing, especially taking into account the abundance of nuclear weapons decommissioning programs and associated challenges with nuclear energy utilization and production.[3,4] As a response to the ever-increasing stockpiles of radionuclide waste, the interest in An-containing systems for gaining fundamental understanding and improving waste repurposing programs has only grown over time.[5–24] In this direction, studies of the physicochemical properties of An-based materials are necessary first steps to build a foundation for beginning to address the current challenges in waste reprocessing by revealing potential applications that have not yet been realized.

High-temperature solid-state reactions have been predominantly used as an experimental approach for preparation of actinide- or transuranic-based materials for systematic studies of material properties.[16,25–29] However, metal–organic frameworks (MOFs) have recently emerged as materials of interest to advance actinide chemistry due to MOFs' diverse structural topologies, porosity, and modularity.[30–34] As expected, the first steps in the relatively novel field of An-MOFs started with the development of synthetic approaches for framework

Department of Chemistry and Biochemistry, University of South Carolina, Columbia, South Carolina 29208, USA. E-mail: shustova@sc.edu

† Electronic supplementary information (ESI) available. See DOI: 10.1039/d1sc01827b

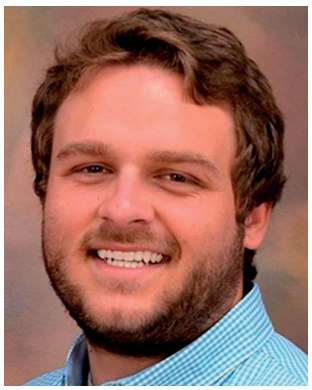

Corey R. Martin is currently pursuing his PhD degree in inorganic chemistry at the University of South Carolina after completing his BA degree in chemistry from Florida Gulf Coast University in 2017. His research interests include the development of novel photo-responsive metal–organic materials for application in optoelectronic devices.

Gabrielle A. Leith is currently pursuing her PhD degree in organic chemistry at the University of South Carolina after completing her BA degree in chemistry from Hanover College in 2017. Her research focuses on designing donor–acceptor fulleretic materials to promote directional charge transfer in a predesigned pathway.

preparation and establishment of methods for their structural characterization.

The inclusion of actinides in MOFs can promote unique properties in comparison with those of well-studied transition metal-based MOFs. For actinides, in general, relativistic effects are substantially more prominent in comparison with transition metals or lanthanides, that can lead to profound spin–orbit coupling.[35–37]

The photophysical properties of An-based materials can be affected by relativistic effects of actinides through mixing of excited and ground states or the relativistic f–f transitions in crystal fields.[38–41] In many cases, theoretical calculations are used to rationalize the structural preferences of the 5f-orbitals in An-based complexes (*e.g.*, $[ThH_6]^{2-}$) relative to the d-orbitals of transition metal-based compounds (*e.g.*, $[HfH_6]^{2-}$).[42] For instance, it was determined that the nature of the *ungerade* f-orbitals found in actinide-containing motifs opens an avenue for structure-bonding that is typically not possible with only *gerade* d-orbitals found in transition metal systems.[42]

Another area of interest is the exceptional stability of actinide-based materials in the presence of ionizing radiation (*i.e.*, high attenuation efficiencies).[43] For example, uranyl-coordination cages, $Li_{12}K_{48}[\{(UO_2)(O_2)\}_{60}(C_2O_4)_{30}]\cdot nH_2O$ and $Li_{24}Na_{24}[(UO_2)_{24}(O_2)_{24}(P_2O_7)_{12}]\cdot 120H_2O$, exhibited stability to both γ- and simulated α-irradiation.[43] In contrast to purely-inorganic compounds that could possess long-term stability to ionizing radiation, it is important to investigate the advantages offered by hybrid systems such as An-MOFs, that could be used for short-term manipulation with radionuclides.[44–46]

Since MOFs can be considered as "bulky linkers" for stabilization of elusive oxidation states, as it was shown on the example of transition metal-based MOFs,[47–49] it is also important to pursue this direction for actinide-containing frameworks. For example, the coordination of actinides in molecular complexes can lead to the stabilization of less-common oxidation states (*e.g.*, Th^{2+}, U^{2+}, and Pu^{2+}).[50–52] Therefore, it is plausible to expect that a framework could allow for isolation of elusive oxidation states that enriches actinide chemistry. Furthermore, high coordination numbers (>14) observed in several examples of An-based organometallic complexes (*e.g.*, $U(BH_4)_4$ and $[Th(H_3BNMe_2BH_3)_4]$)[53–57] could also be achieved through integration of actinides in a MOF. Currently, high coordination numbers (>10) for actinides have already been observed in An-MOFs, suggesting that there is more to be discovered upon further detailed investigations.[53–57]

To summarize, in comparison with the well-explored M-MOF field (M = a transition metal), the instantaneous development of An-MOFs and understanding of their properties (that is the main focus of this perspective, Scheme 1) is mainly impeded by careful implementation of safety protocols. Primarily due to this fact, the first transuranic MOFs have only recently been synthesized.[3,58–60] In general, analysis of reported An-MOF structures has demonstrated that connectivity of the secondary building units (metal nodes) could replicate structural motifs typically observed in natural minerals.[38] At the same time, the An-MOF lattice could support a metal coordination environment that is primarily observed in organometallic complexes.[61–67] For example, the $[U_6O_8]^{8+}$ structural motif found in MOF metal nodes replicates the structure typically observed in actinide-based molecular complexes.[68–75] Similarly, the natural mineral, adolfpateraite, and the $UO_2(OH)(PYCA)$ (HPYCA = pyrazine-2-carboxylic acid) framework both contain similar vertex-sharing pentagonal bipyramidal uranyl metal nodes.[76,77] From this point of view, An-frameworks can be considered a versatile "bridge" between solution and solid-state actinide chemistry.[61] However, actinides integrated within the MOF lattice can also exhibit significantly different behavior in comparison with discrete metal complexes, as demonstrated on the example of cationic exchange reactions.[78] Furthermore,

Natalia B. Shustova is a Professor of Chemistry at the University of South Carolina. She received her MS degree in materials science from Moscow State University (MSU), Russia, PhD degrees in physical chemistry and inorganic chemistry from MSU and Colorado State University, respectively. She completed postdoctoral training at the Massachusetts Institute of Technology. Her research interests span a wide range of topics including sustainable energy conversion, artificial biomimetic systems, actinide chemistry, and stimuli-responsive materials. Her research accolades include the IAS Hans Fischer and Alfred P. Sloan Fellowships and Camille Dreyfus Teaching-Scholar, Cottrell Scholar, and NSF Career Awards.

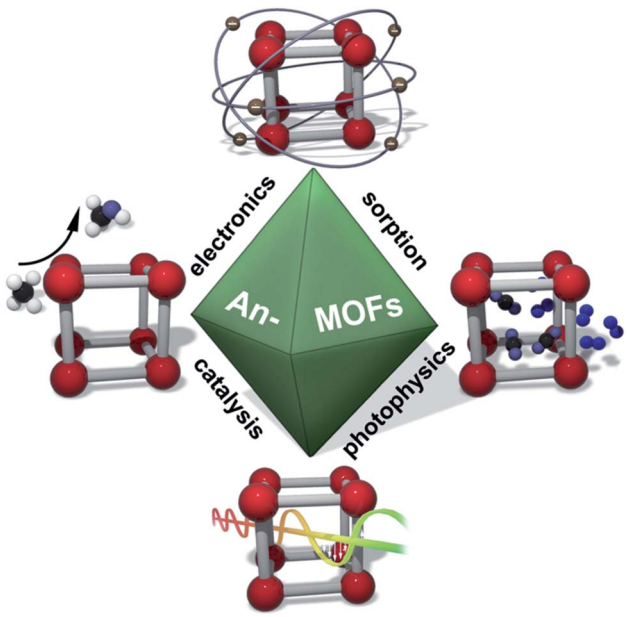

Scheme 1 An overview of the sections related to actinide-containing MOFs discussed in this perspective.

porosity and modularity of MOFs have showcased novel actinide integration methods that are unavailable in other solid-state systems. For instance, a radionuclide can be integrated as a part of a metal node or an organic linker (*e.g.*, capping linkers; Fig. 1) through several approaches such as transmetallation, chelation, or metal node extension.[78] Due to an almost unlimited possibility of combinations of metals and organic linkers, a wide range of structural motifs can be achieved (Fig. 2). Remarkably, some crystalline structures possess exceptionally large unit cell parameters, similar to natural proteins.[79–82] Another unique phenomenon, such as solvent-dependent structural dynamism, was recently reported for Th-MOFs in which the presence of dynamic structural behavior strongly correlated with the coordination number of organic linkers per thorium metal node and was not exhibited by non-radioactive isostructural Zr-containing analogs.[83]

The presented perspective will deviate from outlining exclusively structural aspects, and instead will focus on the remarkable potential of An-MOFs as innovative materials with an emphasis on their physicochemical properties. In particular, we focus on the electronic and photophysical properties of An-frameworks as well as their applications in heterogeneous catalysis and separation (Scheme 1).

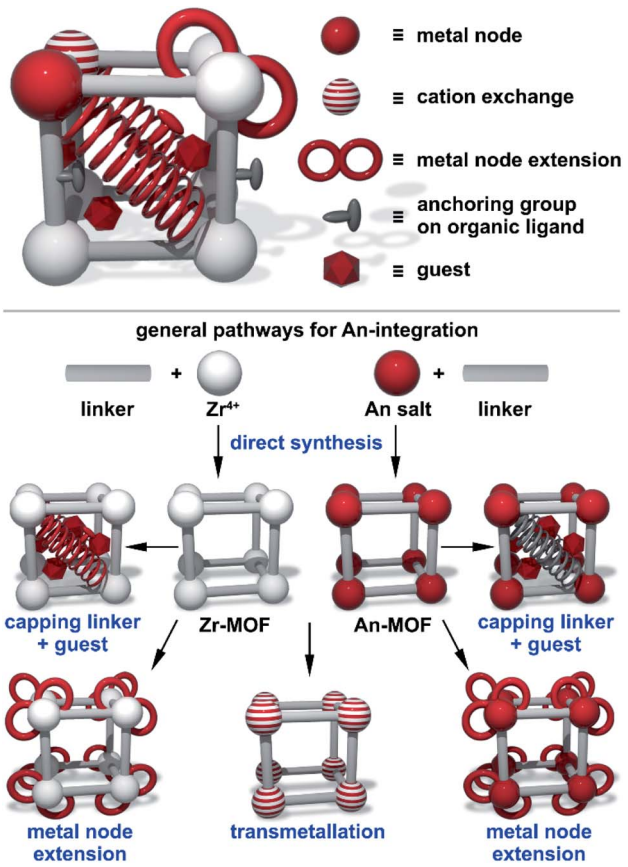

Fig. 1 (Top) A schematic representation of a MOF with pathways for actinide integration highlighted in red. (Bottom) A schematic representation of framework modularity for actinide integration utilizing Zr- and An-based MOFs as precursors. The integrated actinides are displayed in red. Reproduced from ref. 78 with permission from American Chemical Society, Copyright 2017.

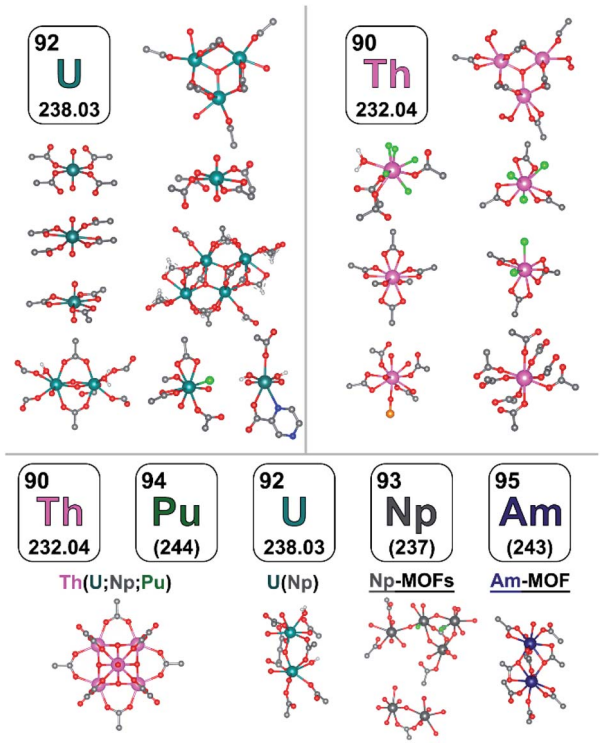

Fig. 2 Secondary building units of several examples of Th, U, Np, Pu, and Am-based MOFs. The teal, pink, dark gray, dark blue, light gray, red, blue, white, and green spheres correspond to uranium, thorium, neptunium, americium, carbon, oxygen, nitrogen, hydrogen, and halogen atoms, respectively.

Electronic properties of An-MOFs

The first section of this perspective focuses on the electronic properties of An-MOFs. Although only a few reports highlight the electronic properties of porous An-based hybrid materials, it has been demonstrated that the role of actinides can make a profound impact on the electronic structures of purely inorganic materials.[84–87] Specifically, unique electronic properties in actinide-containing materials (as opposed to transition metals) arise from relativistic effects resulting in: (1) mixing of electronic ground and excited states and (2) strong spin–orbit coupling.[35]

As previously demonstrated, the electronic properties of MOFs could be controlled "statically" (*i.e.*, through structure modification with metals, linkers, or guests) or "dynamically" (*i.e.*, through application of an external stimulus such as light).[78,83,88,89] The same approaches can be applied towards tailoring the electronic profiles of An-MOFs. Indeed, integration of a thorium cation inside uranium-containing MOFs through cationic exchange can significantly affect the framework's electronic behavior (Fig. 1).[78,83,88] On the example of heterometallic U/Th-MOFs, it was shown that the band gap, estimated from a Tauc plot analysis, decreased from 3.3 eV

($Th_6O_4(OH)_8(Me_2BPDC)_4$; H_2Me_2BPDC = 2,2′-dimethylbiphenyl-4,4′-dicarboxylic acid) to 2.5 eV ($U_{1.23}Th_{4.77}O_4(OH)_8(Me_2BPDC)_4$).[83] The theoretical calculations supported the observed experimental data revealing that uranium integration resulted in changes in the density of states (DOS) near the Fermi edge (E_F). The orbital-projected DOS suggested that orbitals near E_F originated mainly from the uranium 5f-orbitals. Modularity of the frameworks allowed for further tailoring of the Th/U-MOF electronic properties through integration of a transition metal, cobalt, using the metal node extension approach (Fig. 1).[83] Integration of cobalt led to a further decrease of the band gap to 1.9 eV that was also reflected in changes in the calculated DOS of the Th/U/Co-MOF that were primarily dominated by the cobalt 3d-orbitals and oxygen 2p-orbitals.[83] The observed changes in the electronic structures were in-line with conductivity measurements that revealed a three-orders-of-magnitude enhancement from 7.0×10^{-10} S cm^{-1} (Th/U-MOF) to 1.4×10^{-7} S cm^{-1} (Th/U/Co-MOF).[78] Thus, these examples demonstrated that integration of actinides or transition metals can significantly affect the electronic profiles of actinide-containing materials. However, to build a correlation between electronic properties and metal node nuclearity, similar to that reported for transition metal-based MOFs,[90] large samples of data and application of a systematic approach is necessary.

In addition to metal integration, changes in electronic properties of An-frameworks could be made through incorporation of redox-active guests such as 7,7,8,8-tetracyanoquinodimethane (TCNQ) or I_2.[88] For instance, a 50-fold conductivity enhancement was detected for the iodine-doped Th-MOF, I_2@Th-MOF, in comparison with the parent Th-framework.[88]

A next step in tailoring of An-MOF properties is utilizing "dynamic" control through application of an external stimuli (Fig. 3).[89,91–96] To engineer these An-materials, stimuli-responsive components were integrated inside a framework matrix. This approach has been successfully employed on the examples of monometallic Th-MOFs and heterometallic Th/U-MOFs containing spiropyran-based photochromic units (Fig. 3).[88] Spiropyran derivatives are known to exhibit fast and reversible photoisomerization upon alternation of an excitation wavelength in solution.[94] Upon integration into porous An-MOFs, for instance, as a capping linker (Fig. 1), they preserve their photochromic behavior, and as a result, could significantly affect the properties of the framework.[95,96] Indeed, integration of $TNDA^{2-}$ (H_2TNDA = 4,4′-(1′,3′,3′-trimethyl-6-nitrospiro[chromene-2,2′-indoline]-4′,7′-diyl)dibenzoic acid) inside Th- or Th/U-MOFs resulted in significant changes in the DOS of the framework, as demonstrated by theoretical calculations.[88] Indeed, the DOS near E_F of non-photoresponsive monometallic and heterometallic Th- or Th/U-MOFs mainly originated from the 5f orbitals of the metals while upon photochromic unit integration, the frontier orbitals were localized on the photochromic linker.[88] Experimental detection of electronic property modulation upon alternating irradiation with UV and visible light was monitored by changes in conductivity. In addition to optical cycling, alternation of current was observed as shown in Fig. 3.

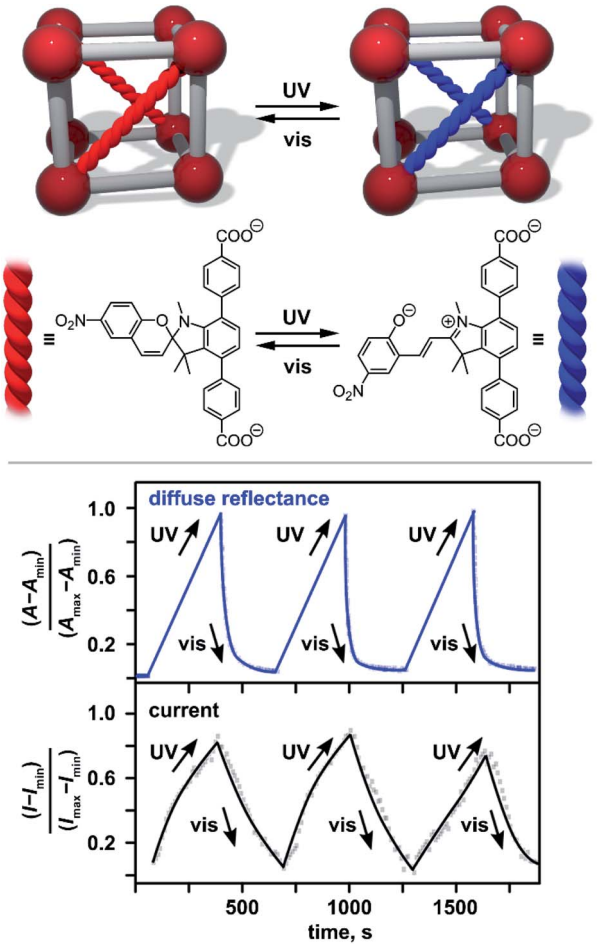

Fig. 3 (Top) Schematic representation of spiropyran photoswitching in Th-based MOFs. (Bottom) Normalized optical and current cycling of photochromic Th-MOF through alternation of UV (λ_{ex} = 365 nm) and visible (λ_{ex} = 590 nm) irradiation. I_{max} and I_{min} = the maximum and minimum current values, respectively; A_{max} and A_{min} = the maximum and minimum absorption values (converted from reflectance *via* the Kubelka–Munk function), respectively. Reproduced from ref. 88 with permission from John Wiley and Sons, Copyright 2021.

As an alternative avenue for tailoring electronic properties of An-MOFs, one can rely on a combination of the aforementioned "static" and "dynamic" approaches.[83,88] For instance, redox-active guest molecules such as TCNQ and I_2 could be integrated inside photochromic An-MOFs.[88] Indeed, modulation of electronic properties upon excitation wavelength alternation was achieved in photochromic Th- and Th/U-MOFs containing TCNQ and I_2 guests, respectively.

As an expansion on actinide-based frameworks with a focus on electronic properties, proton conductivity was measured on the example of a uranyl-containing MOF, $K_2(UO_2)(\mu_3\text{-}O)(BPDSDC)_{0.5}(H_2O)_2$ ($K_2H_2BPDSDC$ = biphenyl-3,3′-disulfonyl-4,4′-dicarboxylic acid dipotassium salt), that exhibited high proton conductivity values due to the decoration of the pores with hydrophilic sulfonate groups (Fig. 4).[97] The highest conductivity value obtained for $K_2(UO_2)(\mu_3\text{-}O)(BPDSDC)_{0.5}(H_2O)_2$ was 1.07×10^{-3} S cm^{-1} at 85 °C (enhanced from $1.27 \times$

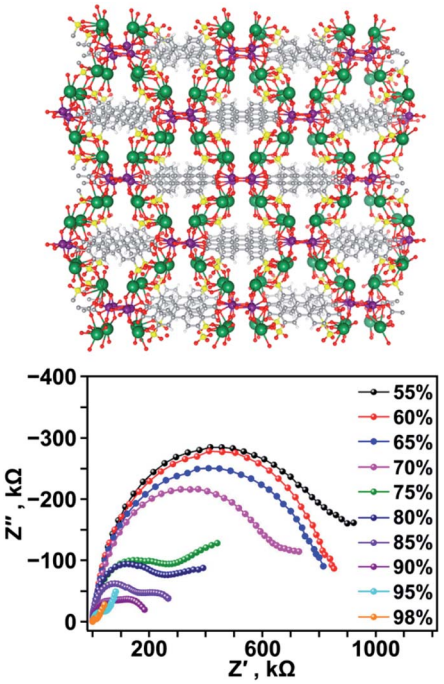

Fig. 4 (Top) X-ray crystal structure of $K_2(UO_2)(\mu_3\text{-}O)(BPDSDC)_{0.5}(H_2O)_2$ and (bottom) Nyquist plots of $K_2(UO_2)(\mu_3\text{-}O)(BPDSDC)_{0.5}(H_2O)_2$ collected under varied relative humidity percentages at 85 °C. The gray, white, yellow, red, purple, and green spheres represent carbon, hydrogen, sulfur, oxygen, uranium, and potassium atoms, respectively. Reproduced from ref. 97 with permission from American Chemical Society, Copyright 2020.

10^{-5} S cm^{-1} at 45 °C). The origin of such behavior was attributed to vehicle-like proton transfer: presence of the sulfonate groups can affect the dynamics of the absorbed water molecules that act as carriers for H^+.[98–101]

As clearly shown based on the reports highlighted in this perspective, studies of An-MOF electronic properties are in their infancy. In contrast to MOFs made of transition metals, where major breakthroughs have already been reported,[102–109] An-MOFs require significant attention from the scientific community. Complimentary to a plethora of crystallographic investigations,[61] computational methods can serve as a reliable and powerful screening tool for the selection of the object of interest, especially taking into account safety protocols required for comprehensive studies of An-MOFs. Currently, theoretical investigations on the electronic properties of An-MOFs are limited to very few reports;[110–112] however, they have already provided several pathways for future investigations that can be crucial for expanding the studies on transuranic MOFs.

An-MOFs for sorption and separation

MOFs are renowned for their sorption and separation capabilities ranging from the removal of harmful biotoxins, long-term storage of energy-relevant gases, charged and neutral organic species separation, and radionuclide sequestration.[113–124] Over the last several decades, trends for designing efficient absorbents based on transition metal-containing MOFs have been preliminarily identified and are still being developed (*e.g.*, high framework flexibility for inert gas capture and separation).[125–131] Large An cations available for MOF synthesis could potentially bring a new flavor to the landscape of MOF-based absorbents and membranes (Fig. 5). For example, adsorption of carbon dioxide in NU-1302 (NU = Northwestern University) resulted in a phase transition.[132] This section will present An-MOFs that have been employed to separate ions (*e.g.*, perrhenate, dichromate, perfluorooctane sulfonate (PFOS), and cesium),[65,133–135] molecular species (*e.g.*, iodine and organic dyes),[136–138] and gases (*e.g.*, carbon dioxide, hydrogen, methane, ethylene, and xenon),[132,139–141] taking into account the possibility of radiation-induced damage in MOFs.[137,142–147]

The interest in MOF-based sorption materials arises from their highly porous nature and the ability to alter a MOFs pore environment through linker functionalization and framework topology.[148–154] Through strategic design of a MOFs metal node and organic linker, metal cations can be exchanged *via* an ion

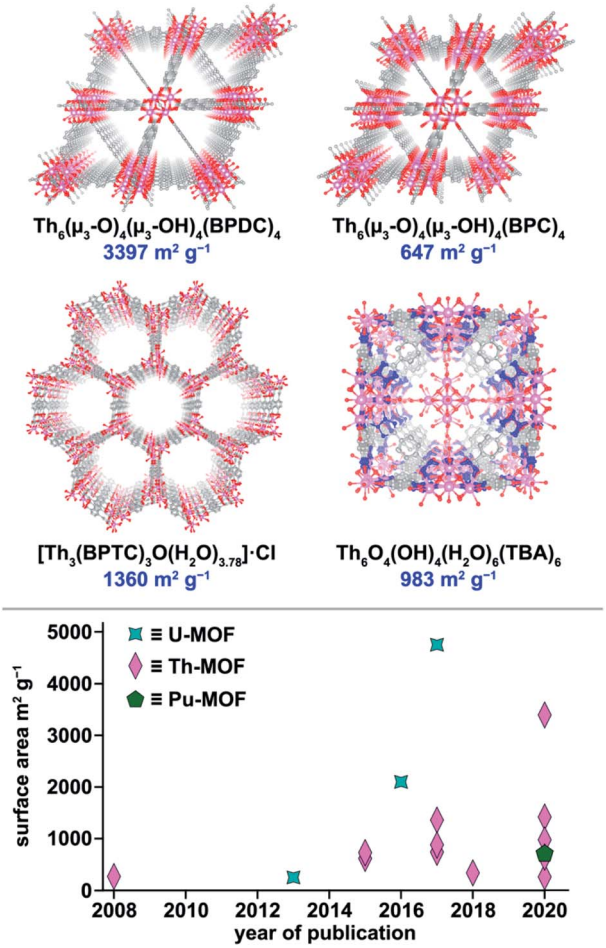

Fig. 5 (Top) X-ray crystal structures of $Th_6(\mu_3\text{-}O)_4(\mu_3\text{-}OH)_4(BPDC)_6$, $Th_6(\mu_3\text{-}O)_4(\mu_3\text{-}OH)_4(BDC)_6$, $[Th_3(BPTC)_3O(H_2O)_{3.78}]\cdot Cl$, and $Th_6O_4(OH)_4(H_2O)_6(TBA)_6$. The pink, blue, gray, and red, spheres represent thorium, nitrogen, carbon, and oxygen atoms, respectively. (Bottom) Literature analysis of the surface areas of several reported An-MOFs over time.[3,59,66,78,134,138,159–163]

metathesis reaction.[155–158] For instance, Shi and coworkers prepared a bipyridinium-based U-containing MOF that was applied for selective removal of perrhenate anions, ReO_4^- (as a non-radioactive surrogate for TcO_4^-).[133] Using $[(UO_2)(BCBP)(OH)(H_2O)]\cdot Cl$ ($[H_2BCBP]Cl_2$ = 1,1′-bis(4-carboxyphenyl)-4,4′-bipyridinium bis(chloride)), the authors were able to achieve a high degree of ReO_4^- sequestration at acidic conditions (86.2% from a 10 mg L^{-1} solution, pH = 4.0). A decrease in pH to 2.0 still resulted in substantial removal of perrhenate anions (63%), foreshadowing practical utilization of the prepared framework for TcO_4^- removal from highly acidic radioactive waste mixtures.[135,164–167]

The first cationic thorium-based framework was recently surveyed for its ability to trap several different types of ions (*e.g.*, polyoxoanions and persistent organic pollutants).[134] The $[Th_3(BPTC)_3O(H_2O)_{3.78}]Cl\cdot(C_5H_{14}N_3Cl)\cdot 8H_2O$ (H_3BPTC = [1,1′-biphenyl]-3,4′,5-tricarboxylic acid) framework was prepared *via* ionothermal synthesis (synthesis in an ionic liquid medium) in tetramethylguanidine chloride at 140 °C.[134] The cationic nature and hydrolytic stability of the Th-based MOF enabled the authors to test its anion-exchange capabilities for perrhenate, dichromate, methyl blue, and PFOS (a persistent organic pollutant). Employment of the Th-MOF resulted in efficient and rapid removal of all of the aforementioned anions. For instance, 80% of ReO_4^- anions and 96% of PFOS were extracted from solution in 2 minutes using the Th-MOF. The authors attributed such high sorption capacity to the cationic nature of the $[Th_3(COO)_9O(H_2O)_3]^+$ metal nodes.[134]

Hierarchical tunability of MOF structures allowed Wang and coworkers to develop a Th-MOF containing a very high void space (74%) and a large surface area (3396.5 $m^2\ g^{-1}$) for radioactive iodine (I^{129} and I^{131}) sequestration[138] as a highly volatile, radiotoxic substance that is detrimental to the human metabolic processes.[168,169] One focus of their report also included the use of modulating acids[170] for efficient control of the MOF growth. The mass uptake of I_2 (gas-phase studies) in the prepared $Th_6(O)_4(OH)_4(H_2O)_6(SBDC)_6$ (H_2SBDC = 4,4′-stilbenedicarboxylic acid) was found to be 1.5 I_2 molecules per Th atom, that is comparable with other MOF-based systems (*e.g.*, 5.3 I_2 molecules per cage in Cu_3BTC_2 (H_3BTC = 1,3,5-benzenetricarboxylic acid)).[171,172] Notably, solution-based sorption studies of iodine in cyclohexane (200 mg L^{-1}) revealed that nearly quantitative iodine removal, using the Th-framework, could be achieved.[138]

As mentioned above, due to high surface areas and the presence of unsaturated metal sites, gas-based sorption and separation are widely studied in MOFs consisting of transition metals.[173–184] Similar studies have also been probed on An-containing frameworks (Fig. 5). By utilizing the pore space of An-MOFs, selective separation of C_2H_4 from a mixture of C_2H_4, C_2H_2, and C_2H_6 was achieved using a Th-based MOF, $Th_6O_4(OH)_4(H_2O)_6(TBA)_6$ ($HTBA$ = 4-(1*H*-tetrazol-5-yl) benzoic acid).[139] This Th-based MOF showed a high adsorption capacity for C_2H_6 (>100.2 $cm^3\ g^{-1}$ at room temperature and 100 kPa), that surpassed the values reported for several other leading transition metal-based porous adsorbents such as $Fe_2(O_2)(DOBDC)$ (H_2DOBDC = 2,5-dioxido-1,4-benzenedicarboxylic acid), Zn(BATZ) (H_2BATZ = bis(5-amino-1*H*-1,2,4-triazol-3-yl) methane), ZIF-7 (ZIF = zeolitic imidazolate framework), ZIF-8, PCN-245 (PCN = porous coordination network), MIL-142A (MIL = Materials Institute Lavoisier), $Cu(Qc)_2$ (HQc = quinoline-5-carboxylic acid), or $Zn_2(ATZ)_2(IPA)$ ($HATZ$ = 3-amino-1,2,4-triazole; H_2IPA = isophthalic acid).[185–192] Compared to C_2H_6, the Th-based MOF had a lower adsorption capacity for C_2H_4 (80.7 $cm^3\ g^{-1}$ at room temperature and 100 kPa) as well as a high adsorption heat enthalpy (28.6 kJ mol^{-1} for C_2H_6) compared to C_2H_2 (25.4 kJ mol^{-1}), that could promote studies for selective C_2H_4 separation from ternary $C_2H_6/C_2H_4/C_2H_2$ mixtures. Along these lines, the authors were also able to purify C_2H_4 (>99.9%) using the Th-based MOF. The proposed mechanism of such behavior in the framework relied on strong van der Waals interactions between C_2H_6 and the MOF skeleton according to DFT calculations.[139]

An important aspect of An-MOFs, that is crucial for a number of the aforementioned applications but especially pertaining to storage/separations, is the stability of frameworks in the presence of ionizing radiation.[137,142–146] Farha and coworkers recently studied radiation-induced damage on the example of two Zr-based MOFs as well as factors that could potentially affect the radiolytic stability such as ligand aromaticity and connectivity, metal node density and connectivity, as well as interligand distance.[146] The authors proposed that differences in the MOF's radiolytic stability could be applied for specific radiological applications (*e.g.*, long-term storage *versus* scintillation sensors). Similarly, Loiseau and coworkers studied the resistance of several MOFs to γ-irradiation.[143] In their study, γ-irradiation (up to 175 Mrad) was applied towards frameworks, followed by extensive characterization using powder X-ray diffraction (PXRD), gas sorption analysis, and nuclear magnetic resonance and fourier-transform infrared spectroscopies. Comprehensive analysis confirmed structural stability after significant γ dosages. In a similar vein, Shustova and coworkers studied γ-irradiation of a Zr-based MOF, $Zr_6O_4(OH)_8(Me_2BPDC)_4$, for a total dose of 19.7 Mrad (209 hours at a dose rate of 94.3 krad $hour^{-1}$), and the MOF still maintained its structural integrity according to crystallographic data.[147]

As clearly demonstrated, these reports have only grazed the surface of storage/separations that could be performed on An-MOFs. More in-depth studies are necessary to highlight the unique role of actinides in sorption processes in which unusual coordination numbers and environments of actinides integrated into a framework lattice could play a significant role (substantially different from ones observed for transition metals).[53–57] High removal capacities of radioactive species in aqueous media using An-frameworks may compete or even surpass other transition metal- or lanthanide-based materials. However, material radioactivity should be taken into account for employment of these materials beyond fundamental studies. For instance, employment of An-MOFs as sorbents for efficient gas separation could be limited due to the required safety protocols. At the same time, the use of radioactive MOFs for targeted sequestration of radioactive species could be a prospective direction for future studies.

Photophysics of An-MOFs

A variety of photophysical studies, which describe Stokes shifts, quantum yields (QYs), lifetimes, effects of external stimuli, and local environment, have been reported for a number of MOF-based systems and is primarily driven by their implementation in programmable sensors, X-ray scintillators, solar cells, photocatalysts, or light-harvesting systems.[89,193–202] A main focus in these studies has been on either specific chromophores (*e.g.*, porphyrin- or boron dipyrromethene-(BODIPY) based linkers)[203–209] integrated inside a MOF matrix or antenna chromophores coupled to lanthanide-containing metal nodes.[210–214] The ability of actinides to support high coordination numbers and a large range of oxidation states (that are different from the properties of transition metals or lanthanides),[12,61,63,215] could result in unique pathways for tailoring photophysical properties. This section of the review will highlight the current progress of photophysical studies on An-MOFs, emphasizing the distinct benefits of MOFs with integrated actinides and pose future possible pathways for material development.

One particular facet of MOF-based photophysics, in which actinide-based MOFs have the capability to stand above the large pool of photoluminescent frameworks, is X-ray scintillation.[199–201] Coupling the porosity, modularity, and luminescent properties of MOFs facilitates their ability to be applied as highly efficient X-ray sensors, as discussed in several reviews.[193,202] For preparing X-ray scintillating materials, in general, a crystalline matrix is typically doped with guest ions that endow the material with luminescent properties to achieve X-ray-to-visible-light conversion.[216–219] Uranium can be considered as a desirable choice for preparation of MOF-based X-ray scintillating materials due to its high atomic number (correlating to a high X-ray attenuation efficiency) in comparison with other natural heavy elements currently used in X-ray scintillators (*e.g.*, lead, tungsten, or thallium).[220] In general, the green emission of uranyl species has been well-documented as a vibrationally-coupled charge-transfer mechanism and has been observed in many systems.[221–223] Owing to these considerations, Wang and coworkers studied X-ray scintillation properties of a uranyl-based MOF as the first MOF-based scintillator with actinide-centered emission.[224] In their report, UO_2(HBTA)(H_2O) (H_3BTA = 1,3,5-benzenetricarboxylic acid) was shown to exhibit an X-ray excited luminescence spectrum nearly identical to that of the UV-excited emission spectrum (Fig. 6). The QY of UO_2(HBTA)(H_2O) was determined to be 58%, that was the highest value among other reported uranyl-containing hybrid materials at that time,[61,65,78,160,161,225–227] including uranyl nitrate (QY = 36%). The observed high QY was attributed to the rigid and dense structure of the U-MOF that restricted non-radiative decay pathways. Moreover, the prepared frameworks demonstrated stability against radiation damage (up to 20 Mrad of radiation; ^{60}Co γ source). The attenuation efficiency of UO_2(HBTA)(H_2O) was notably greater than that of the commercial thallium-doped cesium iodide (CsI:Tl) scintillator, above a photon energy of 20 keV (Fig. 6). The MOF-based material also maintained a substantially lower

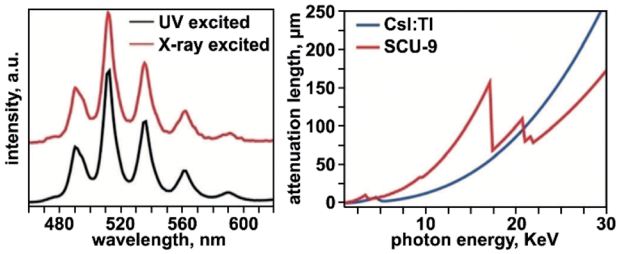

Fig. 6 (Left) Emission profile of UO_2(HBTA)(H_2O) (SCU-9) under UV (black) and X-ray (red) excitation. (Right) X-ray attenuation lengths for UO_2(HBTA)(H_2O) (red) and CsI:Tl (dark blue) in the X-ray energy region ranging from 30 eV to 30 keV. Reproduced from ref. 224 with permission from John Wiley and Sons, Copyright 2018.

structural density (2.88 g cm^{-3} for UO_2(HBTA)(H_2O) and 4.51 g cm^{-3} for CsI:Tl), implying that there is room for improvement as a higher concentration of uranyl units within the lattice may further increase X-ray attenuation efficiency. Thus, given the large attenuation efficiency, high QY, radiation-damage resistance, and lower structural density, these studies highlight the "yet-to-be-revealed" potential for An-MOF-based scintillators that could facilitate changes in the current technological sector.

In a similar vein, Wang and coworkers highlighted the use of a uranyl-based MOF, $(TMA)_2[(UO_2)_4(ox)_4suc]$ (TMA^+ = tetramethylammonium cation; H_2ox = oxalic acid; and H_2suc = succinic acid) as efficient X-ray and γ-irradiation detectors.[227] As a starting point for their studies, they noticed that UV-irradiation of the U-MOF caused emission attenuation, *i.e.*, decreased the emission response over time. Indeed, after only 20 minutes of material irradiation at 365 nm, the emission intensity decreased by 50%, and it was completely quenched after five hours of 365 nm exposure. For emission restoration, the irradiated U-MOF underwent heating at 200 °C for 12 hours. Photoluminescence intensity cycling could also be achieved through alternation of 6 krad γ-irradiation followed by heating. Moreover, exposure of the MOF to only 12 rad of γ-irradiation resulted in a nearly 20% decrease in emission that was four-fold more sensitive than a previously reported solvent-assisted photoluminescence quenching dosimeter.[228–230] Furthermore, exposing the MOF to 10 rad of X-ray led to a 12% decrease in emission intensity.[227]

As mentioned in the first section of this perspective, modulation in photophysical properties of An-MOFs could result in tailoring their electronic properties. To probe this phenomenon, the Shustova research group studied the photochromic properties of An-MOFs with embedded photoresponsive moieties.[88] In particular, one of the focuses of their studies was testing the suitability of different scaffolds to achieve efficient photoisomerization of integrated photochromic diarylethene- and spiropyran units.[96] The latter exhibited limited photoisomerization in the solid state due to constraints imposed by necessary structural rearrangements associated with isomerization processes.[89] However, integration of the abovementioned photoresponsive units inside a porous scaffold resulted in restoration of their photochromic behavior.[96] The

monometallic Th- and heterometallic Th/U-based MOFs were chosen as a platform for tuning of photophysical properties as a function of an excitation wavelength.[88] In particular, diffuse reflectance (DR) measurements showed modulation of absorption profiles upon alternation of UV- and visible light irradiation. Optical cycling showcased the reversibility of photoisomerization processes (Fig. 3). Studies of photoisomerization kinetics allowed for estimation of the attenuation rate of a Th-based spiropyran-containing MOF (3.9×10^{-1} s^{-1}), that is similar to that of a Zr analog (1.5×10^{-1} s^{-1}), and is in line with a previously reported value for a Zn-based spiropyran-containing frameworks (1.6×10^{-1} s^{-1}).[96]

Luminescent MOFs have been readily employed for the creation of sensors and light-emitting diodes;[231–236] however, only recently have they resulted in the preparation of a self-induced radioluminescent system[237] on the example of a Th-MOF, $Th(NDC)_2$ (H_2NDC = 2,6-naphthalenedicarboxylic acid). The $Th(NDC)_2$ framework contains scintillating naphthalene-based struts that are capable of radiation-induced autoluminescence.[237] In the prepared framework, autoluminescence arose from the interactions of the radio emitted ionizing alpha emission from Th^{4+} and the scintillating moiety, NDC^{2-} (Fig. 7). Despite alpha emission, the framework retained crystallinity, even after one year. This noteworthy development emphasizes that harnessing the inherent properties of actinides (*e.g.*, radioactivity) could lead to unconventional avenues for the development of futuristic materials.[231–236]

Another possible pathway for gaining information of An-MOF photophysics, that is worth mentioning in this perspective, is obtaining knowledge from similar actinide-based discrete systems such as metal-coordination cages (MCCs) and then applying that information to extended structures such as MOFs. For example, photoreactivity of UO_2^{2+} was explored on the example of a MCC.[238] An initial uranyl-based cage (tripodal), formed upon reaction of *cis*-calix[4]pyrrole dibenzoic acid with uranyl nitrate and pyridine, underwent conversion to a tetrapodal cage through uranyl-assisted activation of molecular oxygen in the presence of light.[238] Photoreactivity of UO_2^{2+}-based metal nodes coordinated to benzoate groups could be a transformative concept for replication in MOFs possessing similar architectures. In fact, there are a number MOFs with uranyl-containing metal nodes[61,67] and an in-depth photophysical analysis could assist in unveiling their potential.

To summarize, MOF-based photophysics has been reviewed on several occasions,[193–198,239] yet still only a small fraction of reports have focused on the photophysics of An-MOFs beyond recording solely the framework emission spectra. Given the remarkable properties of actinides (*e.g.*, high atomic numbers, high X-ray attenuation, and unique metal coordination environments), photoluminescent An-based MOFs undoubtedly have the capability to cultivate the technological sector. Moreover, fostering a diverse array of investigations is necessary to gain a more comprehensive overview of the An-MOF capabilities.

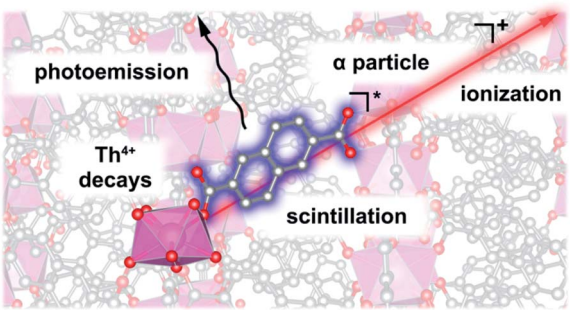

Fig. 7 Autoluminescence in Th_2(NDC) occurring through emission of an alpha particle from a thorium cation, subsequent ionization of the scintillator (NDC^{2-}), followed by core–hole recombination that leaves the system in an electronic excited state, and then visible light photoemission. Reproduced from ref. 237 with permission from American Chemical Society, Copyright 2018.

Heterogenous An-MOF catalysis

Heterogenous catalysis is one of the most widely studied directions for MOFs, as outlined by over a dozen reviews within the last several years.[203–220] The excitement surrounding MOF-based catalysis comes from the intrinsic properties of the frameworks such as the high density of evenly-distributed catalytic active sites, the inherent porous nature, as well as the ability for facile separation of catalyst from products, *e.g.*, *in situ* enantiomeric separations.[240–257] Despite the aforementioned advantages[258] and the potential for small molecule activation using actinide organometallic compounds,[259–272] reports on An-MOF-based catalysis are very limited. For example, there are very few types of reactions (*e.g.*, cycloaddition, dehydrogenation, and photocatalytic oxidation)[57,273–276] that have been probed so far on An-MOFs as heterogeneous catalysts. As a result, there are even fewer reports focused on mechanistic studies of catalytic transformations occurring in An-based MOFs. This section of the review features current An-MOF-based catalysts as well as speculates on the forthcoming discoveries in this promising direction.

In an approach employed by the Farha group, a Th-based MOF, Th-NU-1008 (Fig. 8), was applied as a Lewis acid catalyst, and catalytic activity was examined in comparison with isostructural hexanuclear frameworks containing transition metals, Zr and Hf, and a lanthanide, Ce.[273] The carbon dioxide cyclization into styrene oxide was selected as a model reaction. A 65% conversion of styrene oxide to styrene carbonate after 72 hours was achieved by utilization of Th-NU-1008, while it was surpassed by the Ce-based analog (nearly full conversion in 20 hours). To rationalize the observed catalytic activity (Ce > Zr > Hf > Th for 20 hour reactions), the authors estimated the Lewis acidity of the catalysts by temperature-programmed desorption of ammonia (TPD-NH_3) measurements.[277] However, the established trend Th > Zr > Hf > Ce deviates from the one determined for the catalytic performance that allowed the authors to speculate that other factors rather than Lewis acidity contributed to the reaction progress. One factor that could be responsible for such deviation is terminal water dissociation. For example, dissociation of a water molecule from the cerium-based Lewis sites occurred more rapidly at a lower temperature in

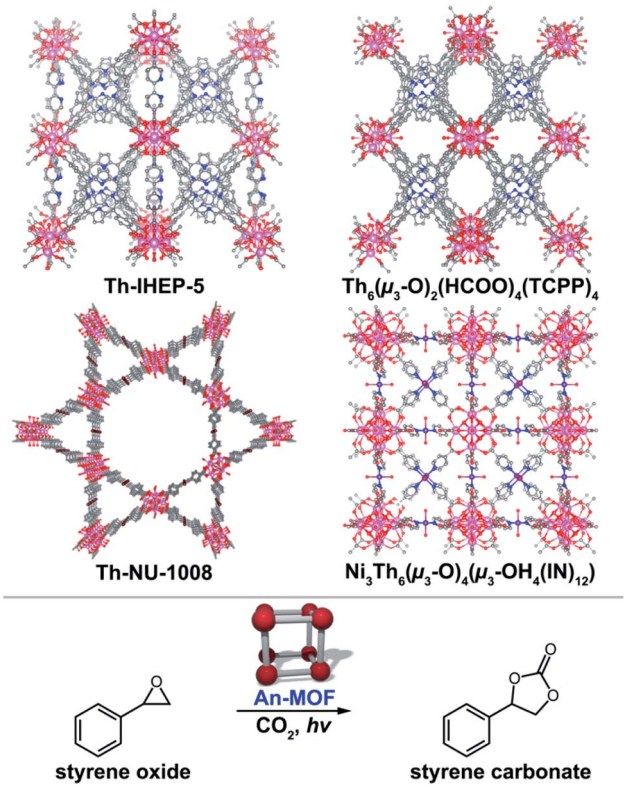

Fig. 8 (Top) X-ray crystal structures of Th-IHEP-5, $Th_6(\mu_3\text{-}O)_2(HCOO)_4(TCPP)_4$, Th-NU-1008, and $Ni_3Th_6(\mu_3\text{-}O)_4(\mu_3\text{-}OH)_4(IN)_{12}\cdot(OH)_6$. The pink, purple, dark red, blue, gray, and red, spheres represent thorium, nickel, bromine, nitrogen, carbon, and oxygen atoms, respectively. (Bottom) A model photocatalytic carbon dioxide cycloaddition reaction that was performed with An-MOFs as a catalyst.[273–276]

comparison with the Th-containing metal nodes.[273] This conclusion was supported by mechanistic studies previously performed for transition metal-containing MOFs.[278] In a similar vein, a mixed-metal Th/Ni-based MOF, $[Ni_3Th_6(\mu_3\text{-}O)_4(\mu_3\text{-}OH)_4(IN)_{12}]\cdot(OH)_6$,[276] was explored for Lewis acid catalysis (Fig. 8). Specifically, a MOF constructed of $Th_{48}Ni_6$ clusters was examined for the photocatalytic carbon dioxide cycloaddition of styrene oxide to styrene carbonate (Fig. 8). For catalytic activity, yields ranged from 89% to 99% (12 hour reaction) using 2-methyloxirane, 2-(chloromethyl)oxirane, 2-(phenoxymethyl) oxirane, 2-((benzyloxy)methyl)oxirane, and 2-phenyloxirane as starting materials. The mechanism of this catalytic reaction was proposed to be mediated by the terminal oxygen atoms of a Th-based metal node with the metal node stabilizing an alkyl-carbonate salt intermediate.[276] The framework also exhibited stability under β-irradiation up to 40 Mrad. As shown in these examples, the unique binding environment of Th- (or U-)[134] containing MOFs could potentially assist in expanding Lewis acid catalysis.[215,279–281]

One of the common organic reactions for testing catalytic properties is the photodegradation of organic dyes (*e.g.*, methyl orange (MO), methyl blue (MB), or rhodamine B (RhB)) which was also explored on several An-MOFs.[282–286] For example, a three-dimensional MOF, $[Na(H_2O)_4][(UO_2)_2Na(FDA)_3(H_2O)_2]$ (H_2FDA = 2,5-furandicarboxylic acid), was capable of decomposing 21.5% of MO after 1.5 hours of UV-irradiation.[284] Similarly, a heterometallic framework, $Ni_2(H_2O)_2(QA)_2(BPy)_2U_5O_{14}(H_2O)_2(OAc)_2$ (H_2QA = quinolinic acid; HOAc = acetic acid), constructed from polyoxouranium ribbons and nickel-based layers bridged by QA^{2-} ligands was employed for photocatalytic degradation of MB.[283] The Chen group synthesized heterometallic MOFs, $Ag(Bipy)(UO_2)(BDC)_{1.5}$ (Bipy = 2,2′-bipyridyl; H_2BDC = 1,4-benzenedicarboxylic acid) and $Ag_2(phen)_2UO_2(BTEC)$ (phen = 1,10-phenanthroline; H_4BTEC = 1,2,4,5-benzenetetracarboxylic acid), and probed them for the photocatalytic degradation of RhB.[287] The authors evaluated the performance of their MOFs against commercial TiO_2 (Degussa P-25) and found that the frameworks displayed photocatalytic activities higher than TiO_2 under UV-irradiation. In particular, a decrease in total organic carbon was 34% and 40% for $Ag(Bipy)(UO_2)(BDC)_{1.5}$ and $Ag_2(phen)_2UO_2(BTEC)$, respectively. The difference in catalytic activity between the two frameworks was mainly attributed to steric hindrance and therefore, the ability for the dye substrate to access the uranium center where catalytic conversion occurred. In addition, $Ag(Bipy)(UO_2)(BDC)_{1.5}$ has a more spacious interlayer area compared to $Ag_2(phen)_2UO_2(BTEC)$, thus making it easier for the dye molecule to diffuse and access the uranium-containing nodes. Interestingly, $Ag(Bipy)(UO_2)(BDC)_{1.5}$ also showed photocatalytic activity under visible light irradiation; however, $Ag_2(phen)_2UO_2(BTEC)$ did not, which was explained by the differences in the absorption profiles of the two MOFs.[287] The reaction was proposed to be catalyzed through photoexcitation of uranium, followed by proton abstraction from RhB. Specifically, a proton is abstracted from the methylene group of RhB, resulting in C–N bond cleavage, and a stepwise *N*-deethylation of RhB.[287] As a follow-up study, the same group designed novel U-based MOFs and probed whether the presence of a transition metal would improve the photocatalytic reaction rate.[285] Irradiation with UV light revealed that two U-based MOFs, $(UO_2)_8(1,4\text{-}NDC)_{12}(4,4'\text{-}BipyH_2)_3(4,4'\text{-}BipyH)_3$ ($1,4\text{-}H_2NDC$ = 1,4-naphthalenedicarboxylic acid) and $(UO_2)_3O[Ag(Bipy)_2]_2(NDC)_3$, would almost quantitatively degrade RhB after 80 minutes, and the use of visible light resulted in degradation of RhB after 10 hours of irradiation. The presence of silver in one of these frameworks, containing a similar amount of uranium (~30%), did not affect the photocatalytic performance, allowing the authors to surmise that the presence of silver was inconsequential in the photocatalytic reactions.

A more recent report utilized MOF modularity to create four U-polycarboxylates frameworks with honeycomb (6,3) nets containing transition metal/phenanthroline complexes or viologen guest molecules to enhance the photodegradation of RhB.[286] The authors discovered that $(MV)[(UO_2)_2(TDC)_3]$ (MV^{2+} = methyl viologen; H_2TDC = thiophene-2,5-dicarboxylic acid) outperformed the other U-based MOFs in this study with almost complete degradation of RhB under visible light irradiation after 60 minutes. The observed photocatalytic performance is suspected to be due to the electron accepting nature of MV^{2+} that can stabilize active peroxide anions that are responsible for

the oxidation of RhB. Overall, this work demonstrated that uranium-based photocatalysts could outperform benchmark materials and showcased An-based MOFs as stable photodegradation catalysts for UV- and visible-irradiation.

The photocatalytic activity of porphyrin-containing An-frameworks was recently reported as a stable and heterogenous alternative to porphyrin-based homogeneous catalysts.[274,275] For example, a U-MOF with integrated porphyrin-based linkers, Co-TCPP (Co-TCPP = Co(II) tetra(4-carboxyphenyl) porphyrin) was used for catalyzing N-heterocycle dehydrogenation reactions.[57] Specifically, dehydration of nine different N-heterocyclic compounds (*e.g.*, 1,2,3,4-tetrahydroquinoline to quinoline) occurred at yields ranging from 61–98%. The authors compared their findings to the activity of a well-known (and structurally similar) homogenous catalyst, Co-TPP (Co-TPP = Co(II) tetraphenyl porphyrin), and determined that the catalytic activity of the Co-based porphyrin MOF was substantially higher (*e.g.*, a 64% yield for Co-TPP and a 93% yield for the MOF). In a similar vein, two porphyrin-based Th-MOFs were probed for the photocatalytic oxidation of 2-chloroethyl ethyl sulfide or the carbon dioxide fixation to styrene oxide.[274] These Th-MOFs were constructed from tetrakis(4-carboxyphenyl)porphyrin ($TCPP^{4-}$) ligands and either 2,2′-bipyridyl-5,5′-dicarboxylate ($BPYDC^{2-}$) or 4,4′-biphenyldicarboxylate ($BPDC^{2-}$) linkers.[274] The $BPYDC^{2-}$-containing Th-MOF, (Th-IHEP-5; Fig. 8), showed 71% photocatalytic conversion of styrene oxide to styrene carbonate after 48 hours; whereas, the $BPDC^{2-}$-containing MOF showed no catalytic activity. Moreover, control experiments performed for each individual organic linker resulted in no product formation. The authors suspected that the bipyridine core of the $BPYDC^{2-}$ linker acted as a photosensitizer and improved the photocatalytic activity of the Th-based porphyrin MOF in the visible region. Since this type of catalytic reaction is influenced by the organic linker, there is uncertainty regarding the role of integrated actinide moieties in comparison with, for instance, well-studied transition metal-based frameworks.[288–290]

The aforementioned results demonstrate the current limitations of the field of heterogeneous catalysis involving An-MOFs. Overall, most reports of An-MOF-based catalysts focused on either the metal site Lewis acidity (that does not surpass the existing MOF-based catalysts) or catalytically-active centers coordinated to the organic linkers rather than the actinide nodes. In contrast, actinide-centered catalysis in organometallic complexes have foreshadowed novel avenues for hydrocarbon photooxidation and photoinduced hydrogen atom abstraction.[259–272] Overall, actinide integration inside a framework lattice could expand the realm of catalytic transformations currently dominated by transition metal-based MOFs and lead to new reactive pathways (through stabilization of unique oxidation states of actinides) or lower activation energy barriers.[47–49,259–272] However, as clearly seen from this section, none of these benefits, as a result of integration of actinides in the MOF lattice, have been demonstrated extensively yet. Therefore, expanding the currently explored routes, that traditionally rely on lanthanides or transition metals, is crucial since it could lead to unexpected results that arise from the unique electronic behavior and possibly reveal cooperative reactivity of actinide-based catalytically active metal nodes and surrounding organic ligands.

Conclusions and perspectives

As featured in this perspective, the field of An-containing MOFs has grown significantly in the past five years, and yet there remains a significant amount of knowledge to discover by preparing unique An-containing motifs. Currently, the An-MOF field has been dominated by thorium- and uranium-containing structures, with only a few reports on transuranic scaffolds.[3,58–60] One of the main challenges that largely impedes the development of the designated field is limited access to actinide-based precursors as well as rigorous safety protocols that are implemented for not only synthetic research groups but also for national facilities where the majority of materials characterization occurs. One could anticipate that the development of stringent safety protocols could facilitate access to transuranic elements beyond national laboratories, leading to the discovery of novel chemical principles or actinide-based materials possessing unprecedented properties. These developments could elevate investigations on transuranic frameworks by addressing fundamental questions regarding their chemical behavior and physicochemical properties. To some extent, this statement is also applicable for the more thoroughly examined uranium- and thorium-containing MOFs. As shown above, each section of this perspective only contains a few examples. For instance, less than five reports discuss the electronic behavior of An-frameworks. Only recently the first photochromic actinide-based frameworks have been synthesized.[88] Along these lines, photophysical studies of actinide-containing MOFs mainly include reports of emission profiles that are essential, but insufficient for the advancement of An-MOF photophysics. Alternatively, a more promising situation is observed in the area related to An-MOF-based sequestration. There are a number of studies demonstrating the suitability of An-MOFs for radionuclide immobilization. Partially, it is due to the enormous previous success achieved for transition metal-based MOFs in the areas of gas storage and separation, that allowed for the research teams to apply similar methods for material analysis of An-containing frameworks. However, it is important to note that the practicality of An-MOF employment as sorbent materials could be very limited due to their radioactive nature. At the same time, sequestration of radioactive species performed on An-MOFs could be one of the areas that will be boosted during the next decade. In terms of catalyst development, An-MOFs have only made their first steps. As expected, only simple transformations have been probed that did not provide a comprehensive overview of possible future directions. Currently, a deficiency of property investigations is due to the relative youth of An-based MOF catalysts that will change as new materials emerge. In particular, small molecule activation was explored on actinide-based molecular complexes[259–272] and could be probed in An-based MOFs that will translate to the overall success of actinides in the sector of heterogeneous catalysis. Development in this area could also result in the

concept proposed above: utilization of radioactive materials for nuclear waste reprocessing.

An area that has barely been explored is the utilization of actinide-containing MOFs for medical applications. Similarly to transition metal-containing MOFs, An-MOFs could be used as targeted drug delivery systems for delivering drugs to tumor tissues.[291] In a similar vein, radioactive transition metals (*e.g.*, ^{99}Tc) have proved successful as metalloradiopharmaceuticals, specifically therapeutic radionuclides that are β- or α-emitters.[292] In particular, a MOF that acted as an α-emitter could potentially be applied in radioactive therapy of, for instance, a malignant tumor.[292] Furthermore, an interesting direction towards radiation-induced autoluminescence of An-MOFs has only been demonstrated on one example.[237]

Another avenue toward the development of An-based radioisotope thermoelectric generators for fueling planetary exploration, currently represented by purely inorganic systems (*e.g.*, US, US_2, U_2S_3, and UN),[293–296] can be expanded through application of recent advances achieved in the MOF field.

Thus, this field of An-MOFs, much like an iceberg where only the surface is exposed, is ripe with opportunity. Especially, taking into account that a MOF is a versatile platform for harnessing the unique properties of these captivating elements. Finding the niche for actinide-containing frameworks is essential for putting An-MOFs on the broad material landscape map.

Author contributions

C. R. M. and G. A. L. conducted the literature research, drafted the manuscript, and designed the figures. N.B. S. conceived the topic and structure of the article as well as secured funding and supervised the completion of the manuscript. All authors reviewed and contributed to this manuscript.

Conflicts of interest

There are no conflicts to declare.

Acknowledgements

N. B. S. gratefully acknowledges the support of the Center for Hierarchical Wasteform Materials (CHWM), an Energy Frontier Research Center funded by the U.S. Department of Energy, Office of Science, Basic Energy Sciences at the University of South Carolina under Award# DE-SC0016574. N. B. S. is also grateful for support from the NSF CAREER Award (DMR-1553634) and a Cottrell Scholar Award from the Research Corporation for Science Advancement. N. B. S. also acknowledges support from the Dreyfus Teaching-Scholar Award supported by the Dreyfus Foundation and the Hans Fischer Fellowship.

Notes and references

1 Z. Chen, P. Li, X. Zhang, M. R. Mian, X. Wang, P. Li, Z. Liu, M. O'Keeffe, J. F. Stoddart and O. K. Farha, *Nano Res.*, 2021, **14**, 376–380.
2 P. Li, X. Wang, K. I. Otake, J. Lyu, S. L. Hanna, T. Islamoglu and O. K. Farha, *ACS Appl. Nano Mater.*, 2019, **2**, 2260–2265.
3 A. M. Hastings, D. Ray, W. Jeong, L. Gagliardi, O. K. Farha and A. E. Hixon, *J. Am. Chem. Soc.*, 2020, **142**, 9363–9371.
4 Y. L. Li, B. D. Zeidman, S. Y. Hu, C. H. Henager, T. M. Besmann and A. Grandjean, *Comput. Mater. Sci.*, 2019, **159**, 103–109.
5 X.-L. Lv, L. Feng, K.-Y. Wang, L.-H. Xie, T. He, W. Wu, J.-R. Li and H.-C. Zhou, *Angew. Chem., Int. Ed.*, 2021, **60**, 2053–2057.
6 S. Yang, D. Streater, C. Fiankor, J. Zhang and J. Huang, *J. Am. Chem. Soc.*, 2021, **143**, 1061–1068.
7 J. Zhang, X. Bu, P. Feng and T. Wu, *Acc. Chem. Res.*, 2020, **53**, 2261–2272.
8 M. Zheng, Y. Wang and P. Feng, *Catalysts*, 2020, **10**, 309.
9 H. Wang, Y. Liu and J. Li, *Adv. Mater.*, 2020, **32**, 2002603.
10 B. Pattengale, D. J. Santalucia, S. Yang, W. Hu, C. Liu, X. Zhang, J. F. Berry and J. Huang, *J. Am. Chem. Soc.*, 2018, **140**, 11573–11576.
11 G. L. Murphy, Y. Wang, P. Kegler, Y. Wang, S. Wang and E. V. Alekseev, *Chem. Commun.*, 2021, **57**, 496–499.
12 P. C. Burns and M. Nyman, *Dalton Trans.*, 2018, **47**, 5916–5927.
13 J. M. Sperling, E. J. Warzecha, C. Celis-Barros, D.-C. Sergentu, X. Wang, B. E. Klamm, C. J. Windorff, A. N. Gaiser, F. D. White, D. A. Beery, A. T. Chemey, M. A. Whitefoot, B. N. Long, K. Hanson, P. Kögerler, M. Speldrich, E. Zurek, J. Autschbach and T. E. Albrecht-Schönzart, *Nature*, 2020, **583**, 396–399.
14 K. Hinz, D. Fellhauer, X. Gaona, M. Vespa, K. Dardenne, D. Schild, T. Yokosawa, M. A. Silver, D. T. Reed, T. E. Albrecht-Schmitt, M. Altmaier and H. Geckeis, *Dalton Trans.*, 2020, **49**, 1570–1581.
15 C. J. Windorff, C. Celis-Barros, J. M. Sperling, N. C. McKinnon and T. E. Albrecht-Schmitt, *Chem. Sci.*, 2020, **11**, 2770–2782.
16 V. Kocevski, C. A. Juillerat, E. E. Moore, H. C. zur Loye and T. M. Besmann, *Cryst. Growth Des.*, 2019, **19**, 966–975.
17 L. Cheng, C. Liang, W. Liu, Y. Wang, B. Chen, H. Zhang, Y. Wang, Z. Chai and S. Wang, *J. Am. Chem. Soc.*, 2020, **142**, 16218–16222.
18 A. N. Hong, H. Yang, A. Zhou, X. Bu and P. Feng, *Cryst. Growth Des.*, 2020, **20**, 6668–6676.
19 S. Tian, S. Xu, J. Liu, C. He, Y. Xiong and P. Feng, *J. Cleaner Prod.*, 2019, **239**, 117767.
20 S. M. Cohen, *Chem. Rev.*, 2012, **112**, 970–1000.
21 M. Kalaj and S. M. Cohen, *ACS Cent. Sci.*, 2020, **6**, 1046–1057.
22 Z. Hu, B. J. Deibert and J. Li, *Chem. Soc. Rev.*, 2014, **43**, 5815–5840.
23 S. E. Gilson, M. Fairley, P. Julien, A. G. Oliver, S. L. Hanna, G. Arntz, O. K. Farha, J. A. Laverne and P. C. Burns, *J. Am. Chem. Soc.*, 2020, **142**, 13299–13304.
24 Y. Wen, P. Zhang, V. K. Sharma, X. Ma and H. C. Zhou, *Cell Rep. Phys. Sci.*, 2021, **2**, 100348.
25 S. Hickam, D. Ray, J. E. S. Szymanowski, R. Y. Li, M. Dembowski, P. Smith, L. Gagliardi and P. C. Burns, *Inorg. Chem.*, 2019, **58**, 12264–12271.

26 M. Autillo and R. E. Wilson, *Inorg. Chem.*, 2019, **58**, 3203–3210.
27 C. A. Juillerat, V. V. Klepov, G. Morrison, K. A. Pace and H.-C. zur Loye, *Dalton Trans.*, 2019, **48**, 3162–3181.
28 G. Morrison, M. S. Christian, T. M. Besmann and H.-C. zur Loye, *J. Phys. Chem. A*, 2020, **124**, 9487–9495.
29 I. Colliard, G. Morrison, H.-C. zur Loye and M. Nyman, *J. Am. Chem. Soc.*, 2020, **142**, 9039–9047.
30 H. Furukawa, K. E. Cordova, M. O'Keeffe and O. M. Yaghi, *Science*, 2013, **341**, 1230444.
31 O. M. Yaghi, M. O'Keeffe, N. W. Ockwig, H. K. Chae, M. Eddaoudi and J. Kim, *Nature*, 2003, **423**, 705–714.
32 C. R. Kim, T. Uemura and S. Kitagawa, *Chem. Soc. Rev.*, 2016, **45**, 3828–3845.
33 S. Dang, Q. L. Zhu and Q. Xu, *Nat. Rev. Mater.*, 2017, **3**, 17075.
34 S. Kitagawa, R. Kitaura and S. I. Noro, *Angew. Chem., Int. Ed.*, 2004, **43**, 2334–2375.
35 M. L. Marsh, F. D. White, S. S. Galley and T. E. Albrecht-Schmitt, *Handb. Phys. Chem. Rare Earths*, 2018, **53**, 1–33.
36 P. Zhang, H. Liu, W. Zou, P. Zhang and S.-X. Hu, *J. Phys. Chem. A*, 2020, **40**, 8173–8183.
37 A. Berning, M. Schweizer, H.-J. Werner, P. J. Knowles and P. Palmieri, *Mol. Phys.*, 2000, **98**, 1823–1833.
38 B. G. Wybourne and L. Smentek, *J. Alloys Compd.*, 2002, **341**, 71–75.
39 L. S. Natrajan, *Coord. Chem. Rev.*, 2012, **256**, 1583–1603.
40 J. G. Tobin, K. T. Moore, B. W. Chung, M. A. Wall, A. J. Schwartz, G. van der Laan and A. L. Kutepov, *Phys. Rev. B: Condens. Matter Mater. Phys.*, 2005, **72**, 085109.
41 M. L. Marsh, F. D. White, S. S. Galley and T. E. Albrecht-Schmitt, *Handb. Phys. Chem. Rare Earths*, 2018, **53**, 1–33.
42 M. Straka, P. Hrobárik and M. Kaupp, *J. Am. Chem. Soc.*, 2005, **127**, 2591–2599.
43 M. Fairley, N. M. Myers, J. E. S. Szymanowski, G. E. Sigmon, P. C. Burns and J. A. LaVerne, *Inorg. Chem.*, 2019, **58**, 14112–14119.
44 Y. Wang, Y. Li, Z. Bai, C. Xiao, Z. Liu, W. Liu, L. Chen, W. He, J. Diwu, Z. Chai, T. E. Albrecht-Schmitt and S. Wang, *Dalton Trans.*, 2015, **44**, 18810–18814.
45 C. Volkringer, N. Henry, S. Grandjean and T. Loiseau, *J. Am. Chem. Soc.*, 2012, **134**, 1275–1283.
46 S. L. Hanna, D. X. Rademacher, D. J. Hanson, T. Islamoglu, A. K. Olszewski, T. M. Nenoff and O. K. Farha, *Ind. Eng. Chem. Res.*, 2020, **59**, 7520–7526.
47 T. Grancha, A. Carné-Sánchez, F. Zarekarizi, L. Hernández-López, J. Albalad, A. Khobotov, V. Guillerm, A. Morsali, J. Juanhuix, F. Gándara, I. Imaz and D. Maspoch, *Angew. Chem., Int. Ed.*, 2021, **60**, 5729–5733.
48 D. M. Shakya, O. A. Ejegbavwo, T. Rajeshumar, S. D. Senanayake, A. J. Brandt, S. Farzandh, N. Acharya, A. M. Ebrahim, A. I. Fenkel, N. Rui, G. L. Tate, J. R. Monnier, K. D. Vogiatzis, N. B. Shustova and D. A. Chen, *Angew. Chem., Int. Ed.*, 2019, **58**, 16533–16537.
49 W. T. K. Chan and W.-T. Wong, *Polyhedron*, 2013, **52**, 43–61.
50 M. R. MacDonald, M. E. Fieser, J. E. Bates, J. W. Ziller, F. Furche and W. J. Evans, *J. Am. Chem. Soc.*, 2013, **135**, 13310–13313.
51 R. R. Langeslay, M. E. Fieser, J. W. Ziller, F. Furche and W. J. Evans, *Chem. Sci.*, 2015, **6**, 517–521.
52 C. J. Windorff, G. P. Chen, J. N. Cross, W. J. Evans, F. Furche, A. J. Gaunt, M. T. Janicke, S. A. Kozimor and B. L. Scott, *J. Am. Chem. Soc.*, 2017, **139**, 3970–3973.
53 T. Arliguie, L. Belkhiri, S.-E. Bouaoud, P. Thuéry, C. Villiers, A. Boucekkine and M. Ephritikhine, *Inorg. Chem.*, 2009, **48**, 221–230.
54 S. R. Daley, P. M. B. Piccoli, A. J. Schultz, T. K. Todorova, L. Gagliardi and G. S. Girolami, *Angew. Chem., Int. Ed.*, 2010, **49**, 3379–3381.
55 S.-X. Hu, P. Zhang, W. Zou and P. Zhang, *Nanoscale*, 2020, **12**, 15054–15065.
56 C. D. Tutson and A. E. V. Gorden, *Coord. Chem. Rev.*, 2017, **333**, 27–43.
57 K.-Q. Hu, Z.-W. Huang, Z.-H. Zhang, L. Mei, B.-B. Qian, J.-P. Yu, Z.-F. Chai and W.-Q. Shi, *Chem.–Eur. J.*, 2018, **24**, 16766–16769.
58 S. E. Gilson, P. Li, J. E. S. Szymanowski, J. White, D. Ray, L. Gagliardi, O. K. Farha and P. C. Burns, *J. Am. Chem. Soc.*, 2019, **141**, 11842–11846.
59 N. P. Martin, J. März, H. Feuchter, S. Duval, P. Roussel, N. Henry, A. Ikeda-Ohno, T. Loiseau and C. Volkringer, *Chem. Commun.*, 2018, **54**, 6979–6982.
60 J. A. Ridenour, R. G. Surbella, A. V. Gelis, D. Koury, F. Poineau, K. R. Czerwinski and C. L. Cahill, *Angew. Chem., Int. Ed.*, 2019, **58**, 16508–16511.
61 E. A. Dolgopolova, A. M. Rice and N. B. Shustova, *Chem. Commun.*, 2018, **54**, 6472–6483.
62 C. Falaise, A. Assen, I. Mihalcea, C. Volkringer, A. Mesbah, N. Dacheux and T. Loiseau, *Dalton Trans.*, 2015, **44**, 2639–2649.
63 Y. Wang, Y. Li, Z. Bai, C. Xiao, Z. Liu, W. Liu, L. Chen, W. He, J. Diwu, Z. Chai, T. E. Albrecht-Schmitt and S. Wang, *Dalton Trans.*, 2015, **44**, 18810–18814.
64 Y. Li, Z. Weng, Y. Wang, L. Chen, D. Sheng, J. Diwu, Z. Chai, T. E. Albrecht-Schmitt and S. Wang, *Dalton Trans.*, 2016, **45**, 918–921.
65 Y. Wang, Z. Liu, Y. Li, Z. Bai, W. Liu, Y. Wang, X. Xu, C. Xiao, D. Sheng, J. Diwu, J. Su, Z. Chai, T. E. Albrecht-Schmitt and S. Wang, *J. Am. Chem. Soc.*, 2015, **137**, 6144–6147.
66 Y. Li, Z. Weng, Y. Wang, L. Chen, D. Sheng, Y. Liu, J. Diwu, Z. Chai, T. E. Albrecht-Schmitt and S. Wang, *Dalton Trans.*, 2015, **44**, 20867–20873.
67 A. J. Lussier, R. A. K. Lopez and P. C. Burns, *Can. Mineral.*, 2016, **54**, 177–283.
68 C. Falaise, A. Assen, I. Mihalcea, C. Volkringer, A. Mesbah, N. Dacheux and T. Loiseau, *Dalton Trans.*, 2015, **44**, 2639–2649.
69 S. Takao, K. Takao, W. Kraus, F. Emmerlink, A. C. Scheinost, G. Bernhard and C. Hennig, *Eur. J. Inorg. Chem.*, 2009, **2009**, 4771–4775.
70 V. Mougel, B. Biswas, J. Pécaut and M. Mazzanti, *Chem. Commun.*, 2010, **46**, 8648–8650.

71 G. Nocton, F. Burdet, J. Pécaut and M. Mazzanti, *Angew. Chem., Int. Ed.*, 2007, **46**, 7574–7578.
72 C. Falaise, C. Volkringer and T. Loiseau, *Cryst. Growth Des.*, 2013, **13**, 3225–3231.
73 C. Hennig, S. Takao, K. Takao, S. Weiss, W. Kraus, F. Emmerling and A. C. Scheinost, *Dalton Trans.*, 2012, **41**, 12818–12823.
74 K. Takao, S. Takao, A. C. Scheinost, G. Bernard and C. Hennig, *Inorg. Chem.*, 2012, **51**, 1336–1344.
75 K. E. Knope and L. Soderholm, *Inorg. Chem.*, 2013, **52**, 6770–6772.
76 R. C. Severance, S. A. Vaughn, M. D. Smith and H.-C. zur Loye, *Solid State Sci.*, 2011, **13**, 1344–1353.
77 J. Plasil, J. Hlousek, F. Veselovsky, K. Fejfarova, M. Dusek, R. Skoda, M. Novak, J. Cejka, J. Sejkora and P. Ondrus, *Am. Mineral.*, 2012, **97**, 447–454.
78 E. A. Dolgopolova, O. A. Ejegbavwo, C. R. Martin, M. D. Smith, W. Setyawan, S. G. Karakalos, C. H. Henager, H.-C. zur Loye and N. B. Shustova, *J. Am. Chem. Soc.*, 2017, **139**, 16852–16861.
79 S. Kato, K. I. Otake, H. Chen, I. Akpinar, C. T. Buru, T. Islamoglu, R. Q. Snurr and O. K. Farha, *J. Am. Chem. Soc.*, 2019, **141**, 2568–2576.
80 S. Wang, Y. Chen, S. Wang, P. Li, C. A. Mirkin and O. K. Farha, *J. Am. Chem. Soc.*, 2019, **141**, 2215–2219.
81 Y. Chen, P. Li, J. A. Modica, R. J. Drout and O. K. Farha, *J. Am. Chem. Soc.*, 2018, **140**, 5678–5681.
82 S. Wang, S. S. Park, C. T. Buru, H. Lin, P. C. Chen, E. W. Roth, O. K. Farha and C. A. Mirkin, *Nat. Commun.*, 2020, **11**, 2495.
83 O. A. Ejegbavwo, C. R. Martin, O. A. Olorunfemi, G. A. Leith, R. T. Ly, A. M. Rice, E. A. Dolgopolova, M. D. Smith, S. G. Karakalos, N. Birkner, B. A. Powell, S. Pandey, R. J. Koch, S. T. Misture, H. C. zur Loye, S. R. Phillpot, K. S. Brinkman and N. B. Shustova, *J. Am. Chem. Soc.*, 2019, **141**, 11628–11640.
84 X.-D. Wen, R. L. Martin, T. M. Henderson and G. E. Scuseria, *Chem. Rev.*, 2013, **113**, 1063–1096.
85 D. E. Bugaris and J. A. Ibers, *Dalton Trans.*, 2010, **39**, 5949–5964.
86 E. Epifano, M. Naji, D. Manara, A. C. Scheinost, C. Hennig, J. Lechelle, R. J. M. Konings, C. Guéneau, D. Prieur, T. Vitova, K. Dardenne, J. Rothe and P. M. Martin, *Commun. Chem.*, 2019, **2**, 59.
87 J. Yao, D. M. Wells, G. H. Chan, H.-Y. Zeng, D. E. Ellis, R. P. Van Duyne and J. A. Ibers, *Inorg. Chem.*, 2008, **47**, 6873–6879.
88 C. R. Martin, G. A. Leith, P. Kittikhunnatham, K. C. Park, O. A. Ejegbavwo, A. Mathur, C. R. Callahan, S. L. Desmond, M. R. Keener, F. Ahmed, S. Pandey, M. D. Smith, S. R. Phillpot, A. B. Greytak and N. B. Shustova, *Angew. Chem., Int. Ed.*, 2021, **60**, 8072–8080.
89 A. M. Rice, C. R. Martin, V. A. Galitskiy, A. A. Berseneva, G. A. Leith and N. B. Shustova, *Chem. Rev.*, 2020, **120**, 8790–8813.
90 O. A. Ejegbavwo, A. A. Berseneva, C. R. Martin, G. A. Leith, S. Pandey, A. J. Brandt, K. C. Park, A. Mathur, S. Farzandh, V. V. Klepov, B. J. Heiser, M. Chandrashekhar, S. G. Karakalos, M. D. Smith, S. R. Phillpot, S. Garashchuk, D. A. Chen and N. B. Shustova, *Chem. Sci.*, 2020, **11**, 7379–7389.
91 S. Castellanos, F. Kapteijn and J. Gascon, *CrystEngComm*, 2016, **18**, 4006–4012.
92 R. Haldar, L. Heinke and C. Wöll, *Adv. Mater.*, 2020, **32**, 1905227.
93 A. B. Kanj, K. Müller and L. Heinke, *Macromol. Rapid Commun.*, 2018, **39**, 1700239.
94 R. Klajn, *Chem. Soc. Rev.*, 2014, **43**, 148–184.
95 E. A. Dolgopolova, V. A. Galitskiy, C. R. Martin, H. N. Gregory, B. J. Yarbrough, A. M. Rice, A. A. Berseneva, O. A. Ejegbavwo, K. S. Stephenson, P. Kittikhunnatham, S. G. Karakalos, M. D. Smith, A. B. Greytak, S. Garashchuk and N. B. Shustova, *J. Am. Chem. Soc.*, 2019, **141**, 5350–5358.
96 D. E. Williams, C. R. Martin, E. A. Dolgopolova, A. Swifton, D. C. Godfrey, O. A. Ejegbavwo, P. J. Pellechia, M. D. Smith and N. B. Shustova, *J. Am. Chem. Soc.*, 2018, **140**, 7611–7622.
97 D.-D. Liu, Y.-L. Wang, F. Luo and Q.-Y. Liu, *Inorg. Chem.*, 2020, **59**, 2952–2960.
98 K.-D. Kreuer, A. Rabenau and W. Weppner, *Angew. Chem., Int. Ed.*, 1982, **21**, 208–209.
99 S. N. Suarez, J. R. P. Jayakody, S. G. Greenbaum, T. Zawodzinski and J. J. Fontanella, *J. Phys. Chem. B*, 2010, **114**, 8941–8947.
100 D.-W. Lim, M. Sadakiyo and H. Kitagawa, *Chem. Sci.*, 2019, **10**, 16–33.
101 G. A. Ludueña, T. D. Kühne and D. Sebastiani, *Chem. Mater.*, 2011, **23**, 1424–1429.
102 T. Chen, J.-H. Dou, L. Yang, C. Sun, N. J. Libretto, G. Skorupskii, J. T. Miller and M. Dinca, *J. Am. Chem. Soc.*, 2020, **142**, 12367–12373.
103 Y. Byun, L. S. Xie, P. Fritz, T. Ashirov, M. Dincă and A. Coskun, *Angew. Chem., Int. Ed.*, 2020, **59**, 15166–15170.
104 R. M. Stolz, A. Mahdavi-Shakib, B. G. Frederick and K. A. Mirica, *Chem. Mater.*, 2020, **32**, 7639–7652.
105 L. Mendecki and K. A. Mirica, *ACS Appl. Mater. Interfaces*, 2018, **10**, 19248–19257.
106 H. Banda, J.-H. Dou, T. Chen, N. J. Libretto, M. Chaudhary, G. M. Bernard, J. T. Miller, V. K. Michaelis and M. Dincă, *J. Am. Chem. Soc.*, 2021, **143**, 2285–2292.
107 M. Ko, L. Mendecki and K. A. Mirica, *Chem. Commun.*, 2018, **54**, 7873–7891.
108 J.-H. Dou, M. Q. Arguilla, Y. Luo, J. Li, W. Zhang, L. Sun, J. L. Mancuso, L. Yang, T. Chen, L. R. Parent, G. Skorupskii, N. J. Libretto, C. Sun, M. C. Yang, P. V. Dip, E. J. Brignole, J. T. Miller, J. Kong, C. H. Hendon, J. Sun and M. Dincă, *Nat. Mater.*, 2021, **20**, 222–228.
109 Z. Meng, R. M. Stolz and K. A. Mirica, *J. Am. Chem. Soc.*, 2019, **141**, 11929–11937.
110 S. Pandey, Z. Jia, B. Demaske, O. A. Ejegbavwo, W. Setyawan, C. H. Henager, N. Shustova and S. R. Phillpot, *J. Phys. Chem. C*, 2019, **123**, 26842–26855.

111 S. Pandey, B. Demaske, O. A. Ejegbavwo, A. A. Berseneva, W. Setyawan, N. Shustova and S. R. Phillpot, *Comput. Mater. Sci.*, 2020, **184**, 109903.
112 L. Li, W. Ma, S. Shen, H. Huang, Y. Bai and H. Liu, *ACS Appl. Mater. Interfaces*, 2016, **8**, 31032–31041.
113 Y. Wu, H. Pang, W. Yao, X. Wang, S. Yu, Z. Yu and X. Wang, *Sci. Bull.*, 2018, **63**, 831–839.
114 C. Xiao, M. A. Silver and S. Wang, *Dalton Trans.*, 2017, **46**, 16381–16386.
115 Y. Belmabkhout, P. M. Bhatt, K. Adil, R. S. Pillai, A. Cadiau, A. Shkurenko, G. Maurin, G. Liu, W. J. Koros and M. Eddaoudi, *Nat. Energy*, 2018, **3**, 1059–1066.
116 Y. Chen, X. Zhang, M. R. Mian, F. A. Son, K. Zhang, R. Cao, Z. Chen, S.-J. Lee, K. B. Idrees, T. A. Goetjen, J. Lyu, P. Li, Q. Xia, Z. Li, J. T. Hupp, T. Islamoglu, A. Napolitano, G. W. Peterson and O. K. Farha, *J. Am. Chem. Soc.*, 2020, **142**, 21428–21438.
117 S. P. Santoso, A. E. Angkawijaya, V. Bundjaja, F. E. Soetaredjo and S. Ismadji, in *Applications of Metal–Organic Frameworks and Their Derived Materials*, Wiley, 2020, pp. 313–355.
118 R. Chen, Z. Yao, N. Han, X. Ma, L. Li, S. Liu, H. Sun and S. Wang, *ACS Omega*, 2020, **5**, 15402–15408.
119 K. Vellingiri, J. E. Szulejko, P. Kumar, E. E. Kwon, K.-H. Kim, A. Deep, D. W. Boukhvalov and R. J. C. Brown, *Sci. Rep.*, 2016, **6**, 27813.
120 Z. Chen, P. Li, R. Anderson, X. Wang, X. Zhang, L. Robison, L. R. Redfern, S. Moribe, T. Islamoglu, D. A. Gómez-Gualdrón, T. Yildirim, J. F. Stoddart and O. K. Farha, *Science*, 2020, **368**, 297–303.
121 N. S. Bobbitt, M. L. Mendonca, A. J. Howarth, T. Islamoglu, J. T. Hupp, O. K. Farha and R. Q. Snurr, *Chem. Soc. Rev.*, 2017, **46**, 3357–3385.
122 M. Woellner, S. Hausdorf, N. Klein, P. Mueller, M. W. Smith and S. Kaskel, *Adv. Mater.*, 2018, **30**, 1704679.
123 T. Islamoglu, Z. Chen, M. C. Wasson, C. T. Buru, K. O. Kirlikovali, U. Afrin, M. R. Mian and O. K. Farha, *Chem. Rev.*, 2020, **120**, 8130–8160.
124 H. Li, K. Wang, Y. Sun, C. T. Lollar, J. Li and H.-C. Zhou, *Mater. Today*, 2018, **21**, 108–121.
125 A. Torrisi, C. Mellot-Draznieks and R. G. Bell, *J. Chem. Phys.*, 2010, **132**, 044705.
126 Z. Li, P. Liu, C. Ou and X. Dong, *ACS Sustainable Chem. Eng.*, 2020, **8**, 15378–15404.
127 D. Banerjee, C. M. Simon, S. K. Elsaidi, M. Haranczyk and P. K. Thallapally, *Chem*, 2018, **4**, 466–494.
128 S. Hiraide, Y. Sakanaka, H. Kajiro, S. Kawaguchi, M. T. Miyahara and H. Tanaka, *Nat. Commun.*, 2020, **11**, 3867.
129 M. V. Parkes, C. L. Staiger, J. J. Perry IV, M. D. Allendorf and J. A. Greathouse, *Phys. Chem. Chem. Phys.*, 2013, **15**, 9093–9106.
130 J. J. Perry, S. L. Teich-Mcgoldrick, S. T. Meek, J. A. Greathouse, M. Haranczyk and M. D. Allendorf, *J. Phys. Chem. C*, 2014, **118**, 11685–11698.
131 G. Feng, Y. Peng, W. Liu, F. Chang, Y. Dai and W. Huang, *Inorg. Chem.*, 2017, **56**, 2363–2366.
132 S. L. Hanna, X. Zhang, K.-I. Otake, R. J. Drout, P. Li, T. Islamoglu and O. K. Farha, *Cryst. Growth Des.*, 2019, **19**, 506–512.
133 L.-W. Zeng, K.-Q. Hu, L. Mei, F.-Z. Li, Z.-W. Huang, S.-W. An, Z.-F. Chai and W.-Q. Shi, *Inorg. Chem.*, 2019, **58**, 14075–14084.
134 Y. Li, Z. Yang, Y. Wang, Z. Bai, T. Zheng, X. Dai, S. Liu, D. Gui, W. Liu, M. Chen, L. Chen, J. Diwu, L. Zhu, R. Zhou, Z. Chai, T. E. Albrecht-Schmitt and S. Wang, *Nat. Commun.*, 2017, **8**, 1354.
135 Z. Bai, Y. Wang, Y. Li, W. Liu, L. Chen, D. Sheng, J. Diwu, Z. Chai, T. E. Albrecht-Schmitt and S. Wang, *Inorg. Chem.*, 2016, **55**, 6358–6360.
136 N. Zhang, Y.-H. Xing and F.-Y. Bai, *Inorg. Chem.*, 2019, **58**, 6866–6876.
137 Z.-J. Li, Z. Yue, Y. Ju, X. Wu, Y. Ren, S. Wang, Y. Li, Z.-H. Zhang, X. Guo, J. Lin and J.-Q. Wang, *Inorg. Chem.*, 2020, **59**, 4435–4442.
138 Z.-J. Li, Y. Ju, B. Yu, X. Wu, H. Lu, Y. Li, J. Zhou, X. Guo, Z.-H. Zhang, J. Lin, J.-Q. Wang and S. Wang, *Chem. Commun.*, 2020, **56**, 6715–6718.
139 Z. Xu, X. Xiong, J. Xiong, R. Krishna, L. Li, Y. Fan, F. Luo and B. Chen, *Nat. Commun.*, 2020, **11**, 3163.
140 Y. Wang, W. Liu, Z. Bai, T. Zheng, M. A. Silver, Y. Li, Y. Wang, X. Wang, J. Diwu, Z. Chai and S. Wang, *Angew. Chem., Int. Ed.*, 2018, **57**, 5783–5787.
141 D. P. Halter, R. A. Klein, M. A. Boreen, B. A. Trump, C. M. Brown and J. R. Long, *Chem. Sci.*, 2020, **11**, 6709–6716.
142 R. N. Widmer, G. I. Lampronti, N. Casati, S. Farsang, T. D. Bennett and S. A. T. Redfern, *Phys. Chem. Chem. Phys.*, 2019, **21**, 12389–12395.
143 C. Volkringer, C. Falaise, P. Devaux, R. Giovine, V. Stevenson, F. Pourpoint, O. Lafon, M. Osmond, C. Jeanjacques, B. Marcillaud, J. C. Sabroux and T. Loiseau, *Chem. Commun.*, 2016, **52**, 12502–12505.
144 S. K. Elsaidi, M. H. Mohamed, A. S. Helal, M. Galanek, T. Pham, S. Suepaul, B. Space, D. Hopkinson, P. K. Thallapally and J. Li, *Nat. Commun.*, 2020, **11**, 3103.
145 J. M. Dorhout, M. P. Wilkerson and K. R. Czerwinski, *J. Radioanal. Nucl. Chem.*, 2019, **320**, 415–424.
146 S. L. Hanna, D. X. Rademacher, D. J. Hanson, T. Islamoglu, A. K. Olszewski, T. M. Nenoff and O. K. Farha, *Ind. Eng. Chem. Res.*, 2020, **59**, 7520–7526.
147 A. A. Berseneva, C. R. Martin, V. A. Galitskiy, O. A. Ejegbavwo, G. A. Leith, R. T. Ly, A. M. Rice, E. A. Dolgopolova, M. D. Smith, H.-C. zur Loye, D. P. DiPrete, J. W. Amoroso and N. B. Shustova, *Inorg. Chem.*, 2020, **59**, 179–183.
148 H. Yang, Y. Wang, R. Krishna, X. Jia, Y. Wang, A. N. Hong, C. Dang, H. E. Castillo, X. Bu and P. Feng, *J. Am. Chem. Soc.*, 2020, **142**, 2222–2227.
149 A. Dinh, H. Yang, F. Peng, T. C. Nguyen, A. Hong, P. Feng and X. Bu, *Cryst. Growth Des.*, 2020, **20**, 3523–3530.
150 Y.-B. Zhang, H. Furukawa, N. Ko, W. Nie, H. J. Park, S. Okajima, K. E. Cordova, H. Deng, J. Kim and O. M. Yaghi, *J. Am. Chem. Soc.*, 2015, **137**, 2641–2650.

151 H. Chen, Z. Chen, L. Zhang, P. Li, J. Liu, L. R. Redfern, S. Moribe, Q. Cui, R. Q. Snurr and O. K. Farha, *Chem. Mater.*, 2019, **31**, 2702–2706.
152 W. Fan, S. Yuan, W. Wang, L. Feng, X. Liu, X. Zhang, X. Wang, Z. Kang, F. Dai, D. Yuan, D. Sun and H.-C. Zhou, *J. Am. Chem. Soc.*, 2020, **142**, 8728–8737.
153 Y. Wang, X. Jia, H. Yang, Y. Wang, X. Chen, A. N. Hong, J. Li, X. Bu and P. Feng, *Angew. Chem., Int. Ed.*, 2020, **59**, 19027–19030.
154 X.-W. Lei, H. Yang, Y. Wang, Y. Wang, X. Chen, Y. Xiao, X. Bu and P. Feng, *Small*, 2020, 2003167.
155 X. Zhao, X. Bu, T. Wu, S.-T. Zheng, L. Wang and P. Feng, *Nat. Commun.*, 2013, **4**, 2344.
156 C. K. Brozek, L. Bellarosa, T. Soejima, T. V. Clark, N. López and M. Dincă, *Chem.–Eur. J.*, 2014, **20**, 6871–6874.
157 A. Chołuj, A. Zieliński, K. Grela and M. J. Chmielewski, *ACS Catal.*, 2016, **6**, 6343–6349.
158 P. He, K.-G. Haw, J. Ren, Q. Fang, S. Qiu and V. Valtchev, *Inorg. Chem. Front.*, 2018, **5**, 2784–2791.
159 C. Falaise, J.-S. Charles, C. Volkringer and T. Loiseau, *Inorg. Chem.*, 2015, **54**, 2235–2242.
160 P. Li, N. A. Vermeulen, X. Gong, C. D. Malliakas, J. F. Stoddart, J. T. Hupp and O. K. Farha, *Angew. Chem., Int. Ed.*, 2016, **55**, 10358–10362.
161 P. Li, N. A. Vermeulen, C. D. Malliakas, D. A. Gómez-Gualdrón, A. J. Howarth, B. L. Mehdi, A. Dohnalkova, N. D. Browning, M. O'Keeffe and O. K. Farha, *Science*, 2017, **356**, 624–627.
162 C. Falaise, C. Volkringer, J.-F. Vigier, N. Henry, A. Beaurain and T. Loiseau, *Chem.–Eur. J.*, 2013, **19**, 5324–5331.
163 K. M. Ok, J. Sung, G. Hu, R. M. J. Jacobs and D. O'Hare, *J. Am. Chem. Soc.*, 2008, **130**, 3762–3763.
164 M. Garai and C. T. Yavuz, *Chem*, 2019, **5**, 750–752.
165 M. Zha, J. Liu, Y.-L. Wong and Z. Xu, *J. Mater. Chem. A*, 2015, **3**, 3928–3934.
166 J. Zhang, L. Chen, X. Dai, L. Zhu, C. Xiao, L. Xu, Z. Zhang, E. V. Alekseev, Y. Wang, C. Zhang, H. Zhang, Y. Wang, J. Diwu, Z. Chai and S. Wang, *Chem*, 2019, **5**, 977–994.
167 Z.-W. Huang, Z.-J. Li, Q.-Y. Wu, L.-R. Zheng, L.-M. Zhou, Z.-F. Chai, X.-L. Wang and W.-Q. Shi, *Environ. Sci.: Nano*, 2018, **5**, 2077–2087.
168 B. J. Riley, J. D. Vienna, D. M. Strachan, J. S. McCloy and J. L. Jerden, *J. Nucl. Mater.*, 2016, **470**, 307–326.
169 J. Huve, A. Ryzhikov, H. Nouali, V. Lalia, G. Augé and T. J. Daou, *RSC Adv.*, 2018, **8**, 29248–29273.
170 A. Schaate, P. Roy, A. Godt, J. Lippke, F. Waltz, M. Wiebcke and P. Behrens, *Chem.–Eur. J.*, 2011, **17**, 6643–6651.
171 D. F. Sava, K. W. Chapman, M. A. Rodriguez, J. A. Greathouse, P. S. Crozier, H. Zhao, P. J. Chupas and T. M. Nenoff, *Chem. Mater.*, 2013, **25**, 2591–2596.
172 D. F. Sava, M. A. Rodriguez, K. W. Chapman, P. J. Chupas, J. A. Greathouse, P. S. Crozier and T. M. Nenoff, *J. Am. Chem. Soc.*, 2011, **133**, 12398–12401.
173 C. E. Bien, K. K. Chen, S.-C. Chien, B. R. Reiner, L.-C. Lin, C. R. Wade and W. S. W. Ho, *J. Am. Chem. Soc.*, 2018, **140**, 12662–12666.
174 Z. Cai, C. E. Bien, Q. Liu and C. R. Wade, *Chem. Mater.*, 2020, **32**, 4257–4264.
175 B. M. Connolly, D. G. Madden, A. E. H. Wheatley and D. Fairen-Jimenez, *J. Am. Chem. Soc.*, 2020, **142**, 8541–8549.
176 Y. Xiao, H. Yang, X. Bu and P. Feng, *Carbon*, 2021, **176**, 421–430.
177 Y. Gu, J.-J. Zheng, K.-I. Otake, M. Shivanna, S. Sakaki, H. Yoshino, M. Ohba, S. Kawaguchi, Y. Wang, F. Li and S. Kitagawa, *Angew. Chem., Int. Ed.*, 2021, **60**, 11688–11694.
178 P. Wu, Y. Li, J.-J. Zheng, N. Hosono, K.-I. Otake, J. Wang, Y. Liu, L. Xia, M. Jiang, S. Sakaki and S. Kitagawa, *Nat. Commun.*, 2019, **10**, 4362.
179 S. Barman, H. Furukawa, O. Blacque, K. Venkatesan, O. M. Yaghi and H. Berke, *Chem. Commun.*, 2010, **46**, 7981–7983.
180 D. Britt, D. Tranchemontagne and O. M. Yaghi, *Proc. Natl. Acad. Sci. U. S. A.*, 2008, **105**, 11623–11627.
181 V. Y. Mao, P. J. Milner, J.-H. Lee, A. C. Forse, E. J. Kim, R. L. Siegelman, C. M. McGuirk, L. B. Porter-Zasada, J. B. Neaton, J. A. Reimer and J. R. Long, *Angew. Chem., Int. Ed.*, 2020, **59**, 19468–19477.
182 A. Jaffe, M. E. Ziebel, D. M. Halat, N. Biggins, R. A. Murphy, K. Chakarawet, J. A. Reimer and J. R. Long, *J. Am. Chem. Soc.*, 2020, **142**, 14627–14637.
183 A. M. Kałuża, S. Mukherjee, S.-Q. Wang, D. J. O'Hearn and M. J. Zaworotko, *Chem. Commun.*, 2020, **56**, 1940–1943.
184 H. Li, L. Li, R.-B. Lin, W. Zhou, Z. Zhang, S. Xiang and B. Chen, *EnergyChem*, 2019, **1**, 100006.
185 K.-J. Chen, D. G. Madden, S. Mukherjee, T. Pham, K. A. Forrest, A. Kumar, B. Space, J. Kong, Q.-Y. Zhang and M. J. Zaworotko, *Science*, 2019, **366**, 241–246.
186 R.-B. Lin, H. Wu, L. Li, X.-L. Tang, Z. Li, J. Gao, H. Cui, W. Zhou and B. Chen, *J. Am. Chem. Soc.*, 2018, **140**, 12940–12946.
187 L. Li, R.-B. Lin, R. Krishna, H. Li, S. Xiang, H. Wu, J. Li, W. Zhou and B. Chen, *Science*, 2018, **362**, 443–446.
188 Y. Wu, H. Chen, D. Liu, Y. Qian and H. Xi, *Chem. Eng. Sci.*, 2015, **124**, 144–153.
189 D.-L. Chen, N. Wang, C. Xu, G. Tu, W. Zhu and R. Krishna, *Microporous Mesoporous Mater.*, 2015, **208**, 55–65.
190 D. Lv, R. Shi, Y. Chen, Y. Wu, H. Wu, H. Xi, Q. Xia and Z. Li, *ACS Appl. Mater. Interfaces*, 2018, **10**, 8366–8373.
191 Y. Chen, H. Wu, D. Lv, R. Shi, Y. Chen, Q. Xia and Z. Li, *Ind. Eng. Chem. Res.*, 2018, **57**, 4063–4069.
192 P.-Q. Liao, W.-X. Zhang, J.-P. Zhang and X.-M. Chen, *Nat. Commun.*, 2015, **6**, 8697.
193 E. A. Dolgopolova, A. M. Rice, C. R. Martin and N. B. Shustova, *Chem. Soc. Rev.*, 2018, **47**, 4710–4728.
194 Q. Wang, Q. Gao, A. M. Al-Enizi, A. Nafady and S. Ma, *Inorg. Chem. Front.*, 2020, **7**, 300–339.
195 C. R. Martin, P. Kittikhunnatham, G. A. Leith, A. A. Berseneva, K. C. Park, A. B. Greytak and N. B. Shustova, *Nano Res.*, 2021, **14**, 338–354.
196 T. N. Nguyen, F. M. Ebrahim and K. C. Stylianou, *Coord. Chem. Rev.*, 2018, **377**, 259–306.

197 G. A. Leith, C. R. Martin, J. M. Mayers, P. Kittikhunnatham, R. W. Larsen and N. B. Shustova, *Chem. Soc. Rev.*, 2021, **50**, 4382–4410.
198 Z. Zhuang and D. Liu, *Nano-Micro Lett.*, 2020, **12**, 132.
199 J. Lu, X.-H. Xin, Y.-J. Lin, S.-H. Wang, J.-G. Xu, F.-K. Zheng and G.-C. Guo, *Dalton Trans.*, 2019, **48**, 1722–1731.
200 X. Wang, Y. Wang, Y. Wang, H. Liu, Y. Zhang, W. Liu, X. Wang and S. Wang, *Chem. Commun.*, 2020, **56**, 233–236.
201 F. P. Doty, C. A. Bauer, A. J. Skulan, P. G. Grant and M. D. Allendorf, *Adv. Mater.*, 2009, **21**, 95–101.
202 C. Wang, O. Volotskova, K. Lu, M. Ahmad, C. Sun, L. Xing and W. Lin, *J. Am. Chem. Soc.*, 2014, **136**, 6171–6174.
203 A. Aziz, A. R. Ruiz-Salvador, N. C. Hernández, S. Calero, S. Hamad and R. Grau-Crespo, *J. Mater. Chem. A*, 2017, **5**, 11894–11904.
204 Z. Zhou, S. Mukherjee, J. Warnan, W. Li, S. Wannapaiboon, S. Hou, K. Rodewald, B. Rieger, P. G. Weidler, C. Wöll and R. A. Fischer, *J. Mater. Chem. A*, 2020, **8**, 25941–25950.
205 S. M. Pratik, L. Gagliardi and C. J. Cramer, *J. Phys. Chem. C*, 2020, **124**, 1878–1887.
206 H. Yang, J. Wang, J. Ma, H. Yang, J. Zhang, K. Lv, L. Wen and T. Peng, *J. Mater. Chem. A*, 2019, **7**, 10439–10445.
207 H. Yang, M. Zhao, J. Zhang, J. Ma, P. Wu, W. Liu and L. Wen, *J. Mater. Chem. A*, 2019, **7**, 20742–20749.
208 C. Y. Lee, O. K. Farha, B. J. Hong, A. A. Sarjeant, S. T. Nguyen and J. T. Hupp, *J. Am. Chem. Soc.*, 2011, **133**, 15858–15861.
209 J. Chen, Y. Zhu and S. Kaskel, *Angew. Chem., Int. Ed.*, 2021, **60**, 5010–5035.
210 T. Sun, Y. Gao, Y. Du, L. Zhou and X. Chen, *Front. Chem.*, 2021, **8**, 624592.
211 B. Yan, *Acc. Chem. Res.*, 2017, **50**, 2789–2798.
212 L. V. Meyer, F. Schönfeld and K. Müller-Buschbaum, *Chem. Commun.*, 2014, **50**, 8093–8108.
213 A. Foucault-Collet, K. A. Gogick, K. A. White, S. Villette, A. Pallier, G. Collet, C. Kieda, T. Li, S. J. Geib, N. L. Rosi and S. Petoud, *Proc. Natl. Acad. Sci. U. S. A.*, 2013, **110**, 17199–17204.
214 N. Wu, H. Guo, X. Wang, L. Sun, T. Zhang, L. Peng and W. Yang, *Colloids Surf., A*, 2020, **616**, 126093.
215 T. Islamoglu, A. Atilgan, S.-Y. Moon, G. W. Peterson, J. B. DeCoste, M. Hall, J. T. Hupp and O. K. Farha, *Chem. Mater.*, 2017, **29**, 2672–2675.
216 P. Lecoq, *Nucl. Instrum. Methods Phys. Res., Sect. A*, 2016, **809**, 130–139.
217 M. D. Birowosuto, D. Cortecchia, W. Drozdowski, K. Brylew, W. Lachmanski, A. Bruno and C. Soci, *Sci. Rep.*, 2016, **6**, 37254.
218 W. Zhu, W. Ma, Y. Su, Z. Chen, X. Chen, Y. Ma, L. Bai, W. Xiao, T. Liu, H. Zhu, X. Liu, H. Liu, X. Liu and Y. Yang, *Light: Sci. Appl.*, 2020, **9**, 112.
219 F. Zhou, Z. Li, W. Lan, Q. Wang, L. Ding and Z. Jin, *Small Methods*, 2020, **4**, 2000506.
220 G. Liu and J. V. Beitz, *The Chemistry of the Actinide and Transactinide Elements*, Springer, Heidelberg, 2006.
221 G. Liu, N. P. Deifel, C. L. Cahill, V. V. Zhurov and A. A. Pinkerton, *J. Phys. Chem. A*, 2012, **116**, 855–864.
222 S. Tsushima, C. Götz and K. Fahmy, *Chem.–Eur. J.*, 2010, **16**, 8029–8033.
223 M. C. Phillips, B. E. Brumfield, N. LaHaye, S. S. Harilal, K. C. Hartig and I. Jovanovic, *Sci. Rep.*, 2017, **7**, 3784.
224 Y. Wang, X. Yin, W. Liu, J. Xie, J. Chen, M. A. Silver, D. Sheng, L. Chen, J. Diwu, N. Liu, Z. Chai, T. E. Albrecht-Schmitt and S. Wang, *Angew. Chem., Int. Ed.*, 2018, **57**, 7883–7887.
225 K.-X. Wang and J.-S. Chen, *Acc. Chem. Res.*, 2011, **44**, 531–540.
226 C. Volkringer, N. Henry, S. Grandjean and T. Loiseau, *J. Am. Chem. Soc.*, 2012, **134**, 1275–1283.
227 J. Xie, Y. Wang, W. Liu, X. Yin, L. Chen, Y. Zou, J. Diwu, Z. Chai, T. E. Albrecht-Schmitt, G. Liu and S. Wang, *Angew. Chem., Int. Ed.*, 2017, **56**, 7500–7504.
228 J.-M. Han, M. Xu, B. Wang, N. Wu, X. Yang, H. Yang, B. J. Salter and L. Zang, *J. Am. Chem. Soc.*, 2014, **136**, 5090–5096.
229 X. Dong, F. Hu, Z. Liu, G. Zhang and D. Zhang, *Chem. Commun.*, 2015, **51**, 3892–3895.
230 J.-M. Han, N. Wu, B. Wang, C. Wang, M. Xu, X. Yang, H. Yang and L. Zang, *J. Mater. Chem. C*, 2015, **3**, 4345–4351.
231 X.-Y. Liu, W. P. Lustig and J. Li, *ACS Energy Lett.*, 2020, **5**, 2671–2680.
232 W. P. Lustig, F. Wang, S. J. Teat, Z. Hu, Q. Gong and J. Li, *Inorg. Chem.*, 2016, **55**, 7250–7256.
233 G. E. Gomez, R. Marin, A. N. Carneiro Neto, A. M. P. Botas, J. Ovens, A. A. Kitos, M. C. Bernini, L. D. Carlos, G. J. A. A. Soler-Illia and M. Murugesu, *Chem. Mater.*, 2020, **32**, 7458–7468.
234 T. Mondal, S. Mondal, S. Bose, D. Sengupta, U. K. Ghorai and S. K. Saha, *J. Mater. Chem. C*, 2018, **6**, 614–621.
235 A. Khatun, D. K. Panda, N. Sayresmith, M. G. Walter and S. Saha, *Inorg. Chem.*, 2019, **58**, 12707–12715.
236 Y. Shu, Q. Ye, T. Dai, Q. Xu and X. Hu, *ACS Sens.*, 2021, **6**, 641–658.
237 J. Andreo, E. Priola, G. Alberto, P. Benzi, D. Marabello, D. M. Proserpio, C. Lamberti and E. Diana, *J. Am. Chem. Soc.*, 2018, **140**, 14144–14149.
238 J. Lee, J. T. Brewster, B. Song, V. M. Lynch, I. Hwang, X. Li and J. L. Sessler, *Chem. Commun.*, 2018, **54**, 9422–9425.
239 M. C. So, G. P. Wiederrecht, J. E. Mondloch, J. T. Hupp and O. K. Farha, *Chem. Commun.*, 2015, **51**, 3501–3510.
240 J. Lee, O. K. Farha, J. Roberts, K. A. Scheidt, S. T. Nguyen and J. T. Hupp, *Chem. Soc. Rev.*, 2009, **38**, 1450–1459.
241 K. Shen, X. Chen, J. Chen and Y. Li, *ACS Catal.*, 2016, **6**, 5887–5903.
242 Y.-B. Huang, J. Liang, X.-S. Wang and R. Cao, *Chem. Soc. Rev.*, 2017, **46**, 126–157.
243 Y.-Z. Chen, R. Zhang, L. Jiao and H.-L. Jiang, *Coord. Chem. Rev.*, 2018, **362**, 1–23.
244 J. Liu, L. Chen, H. Cui, J. Zhang, L. Zhang and C.-Y. Su, *Chem. Soc. Rev.*, 2014, **43**, 6011–6061.
245 B. Li, M. Chrzanowski, Y. Zhang and S. Ma, *Coord. Chem. Rev.*, 2016, **307**, 106–129.
246 A. Dhakshinamoorthy, M. Alvaro and H. Garcia, *Chem. Commun.*, 2012, **48**, 11275–11288.

247 P. García-García, M. Müller and A. Corma, *Chem. Sci.*, 2014, **5**, 2979–3007.
248 V. Bernales, M. A. Ortuño, D. G. Truhlar, C. J. Cramer and L. Gagliardi, *ACS Cent. Sci.*, 2018, **4**, 5–19.
249 J. Gascon, A. Corma, F. Kapteijn and F. X. Llabreés i Xamena, *ACS Catal.*, 2014, **4**, 361–378.
250 D. Farrusseng, S. Aguado and C. Pinel, *Angew. Chem., Int. Ed.*, 2009, **48**, 7502–7513.
251 A. Dhakshinamoorthy, M. Alvaro, A. Corma and H. Garcia, *Dalton Trans.*, 2011, **40**, 6344–6360.
252 A. Corma, H. García and F. X. Llabrés i Xamena, *Chem. Rev.*, 2010, **110**, 4606–4655.
253 A. H. Chughtai, N. Ahmad, H. A. Younus, A. Laypkov and F. Verpoort, *Chem. Soc. Rev.*, 2015, **44**, 6804–6849.
254 Q. Yang, Q. Xu and H.-L. Jiang, *Chem. Soc. Rev.*, 2017, **46**, 4774–4808.
255 L. Zhu, X.-Q. Liu, H.-L. Jiang and L.-B. Sun, *Chem. Rev.*, 2017, **117**, 8129–8176.
256 L. Ma, C. Abney and W. Lin, *Chem. Soc. Rev.*, 2009, **38**, 1248–1256.
257 S.-N. Zhao, X.-Z. Song, S.-Y. Song and H.-J. Zhang, *Coord. Chem. Rev.*, 2017, **337**, 80–96.
258 M. Fujita, Y. J. Kwon, S. Washizu and K. Ogura, *J. Am. Chem. Soc.*, 1994, **116**, 1151–1152.
259 W.-D. Wang, A. Bakac and J. H. Espenson, *Inorg. Chem.*, 1995, **34**, 6034–6039.
260 Y. Mao and A. Bakac, *J. Phys. Chem.*, 1996, **100**, 4219–4223.
261 H. D. Burrows and T. J. Kemp, *Chem. Soc. Rev.*, 1974, **3**, 139–165.
262 S. G. Thangavelu and C. L. Cahill, *Inorg. Chem.*, 2015, **54**, 4208–4221.
263 J. August Ridenour and C. L. Cahill, *New J. Chem.*, 2018, **42**, 1816–1831.
264 J. Leduc, M. Frank, L. Jürgensen, D. Graf, A. Raauf and S. Mathur, *ACS Catal.*, 2019, **9**, 4719–4741.
265 J. G. West, T. A. Bedell and E. J. Sorensen, *Angew. Chem., Int. Ed.*, 2016, **55**, 8923–8927.
266 B. T. McGrail, L. S. Pianowski and P. C. Burns, *J. Am. Chem. Soc.*, 2014, **136**, 4797–4800.
267 Y. Mao and A. Bakac, *Inorg. Chem.*, 1996, **35**, 3925–3930.
268 T. M. McCleskey, C. J. Burns and W. Tumas, *Inorg. Chem.*, 1999, **38**, 5924–5925.
269 R. Nagaishi, Y. Katsumura, K. Ishigure, H. Aoyagi, Z. Yoshida, T. Kimura and Y. Kato, *J. Photochem. Photobiol., A*, 2002, **146**, 157–161.
270 G. M. Kramer, M. B. Dines, A. Kaldor, R. Hall and D. McClure, *Inorg. Chem.*, 1981, **20**, 1421–1426.
271 C. Miyake, Y. Yamana, S. Imoto and H. Ohya-Nishiguchi, *Inorg. Chim. Acta*, 1984, **95**, 17–21.
272 C. K. Rofer-DePoorter and G. L. DePoorter, *J. Inorg. Nucl. Chem.*, 1977, **39**, 631–634.
273 J. Lyu, X. Zhang, P. Li, X. Wang, C. T. Buru, P. Bai, X. Guo and O. K. Farha, *Chem. Mater.*, 2019, **31**, 4166–4172.
274 Z.-W. Huang, K.-Q. Hu, L. Mei, X.-H. Kong, J.-P. Yu, K. Liu, L.-W. Zeng, Z.-F. Chai and W.-Q. Shi, *Dalton Trans.*, 2020, **49**, 983–987.
275 P. Li, S. Goswami, K.-I. Otake, X. Wang, Z. Chen, S. L. Hanna and O. K. Farha, *Inorg. Chem.*, 2019, **58**, 3586–3590.
276 H. Xu, C.-S. Cao, H.-S. Hu, S.-B. Wang, J.-C. Liu, P. Cheng, N. Kaltsoyannis, J. Li and B. Zhao, *Angew. Chem., Int. Ed.*, 2019, **58**, 6022–6027.
277 R. D. Shannon and C. T. Prewitt, *Acta Crystallogr., Sect. B: Struct. Crystallogr. Cryst. Chem.*, 1969, **25**, 925–946.
278 J. Kim, S.-N. Kimg, H.-G. Jang, G. Seo and W.-S. Ahn, *Appl. Catal., A*, 2013, **453**, 175–180.
279 M. H. Beyzavi, C. J. Stephenson, Y. Liu, O. Karagiaridi, J. T. Hupp and O. K. Farha, *Front. Energy Res.*, 2015, **2**, 1–10.
280 J. E. Mondloch, M. J. Katz, W. C. Isley, P. Ghosh, P. Liao, W. Bury, G. W. Wagner, M. G. Hall, J. B. DeCoste, G. W. Peterson, R. Q. Snurr, C. J. Cramer, J. T. Hupp and O. K. Farha, *Nat. Mater.*, 2015, **14**, 512–516.
281 M. H. Beyzavi, R. C. Klet, S. Tussupbayev, J. Borycz, N. A. Vermeulen, C. J. Cramer, J. F. Stoddart, J. T. Hupp and O. K. Farha, *J. Am. Chem. Soc.*, 2014, **136**, 15861–15864.
282 S. J. Jennifer and A. K. Jana, *Cryst. Growth Des.*, 2017, **17**, 5318–5329.
283 Z.-T. Yu, Z.-L. Liao, Y.-S. Jiang, G.-H. Li, G.-D. Li and J.-S. Chen, *Chem. Commun.*, 2004, 1814–1815.
284 H. Wang, Z. Chang, Y. Li, R.-M. Wen and X.-H. Bu, *Chem. Commun.*, 2013, **49**, 6659–6661.
285 Z.-L. Liao, G.-D. Li, M.-H. Bi and J.-S. Chen, *Inorg. Chem.*, 2008, **47**, 4844–4853.
286 H.-H. Li, X.-H. Zeng, H.-Y. Wu, X. Jie, S.-T. Zheng and Z.-R. Chen, *Cryst. Growth Des.*, 2015, **15**, 10–13.
287 Z.-T. Yu, Z.-L. Liao, Y.-S. Jiang, G.-H. Li and J.-S. Chen, *Chem.–Eur. J.*, 2005, **11**, 2642–2650.
288 P. Ji, X. Feng, P. Oliveres, Z. Li, A. Murakami, C. Wang and W. Lin, *J. Am. Chem. Soc.*, 2019, **141**, 14878–14888.
289 K. Epp, A. L. Semrau, M. Cokoja and R. A. Fischer, *ChemCatChem*, 2018, **10**, 3506–3512.
290 Z. Hu and D. Zhao, *CrystEngComm*, 2017, **19**, 4066–4081.
291 M. Cai, G. Chen, L. Qin, C. Qu, X. Dong, J. Ni and X. Yin, *Pharmaceutics*, 2020, **12**, 232.
292 E. Boros and A. B. Packard, *Chem. Rev.*, 2019, **119**, 870–901.
293 I. H. Warren and C. E. Price, *Can. Metall. Q.*, 1964, **3**, 183–196.
294 M. Kamimoto, Y. Takahashi and T. Mukaibo, *J. Nucl. Mater.*, 1976, **59**, 149–157.
295 R. Didchenko and F. P. Gortsema, *Inorg. Chem.*, 1963, **2**, 1079–1080.
296 I. H. Warren and C. E. Price, *Can. Metall. Q.*, 1964, **3**, 245–256.